NTNU – Trondheim
Norwegian University of
Science and Technology

Long-Term Wave Power Statistics for Individual Waves

Børge Sveaas Skøyen

Marine Technology
Submission date: June 2012
Supervisor: Dag Myrhaug, IMT
Co-supervisor: Bernt Johan Leira, IMT

Norwegian University of Science and Technology
Department of Marine Technology

NTNU Trondheim
Norwegian University of Science and Technology
Department of Marine Technology

MASTER THESIS IN MARINE TECHNOLOGY

SPRING 2012

FOR

STUD. TECHN. BØRGE SVEAAS SKØYEN

LONG-TERM WAVE POWER STATISTICS FOR INDIVIDUAL WAVES

Ocean wave energy appears to be promising as a source of alternative energy. The design of appropriate devices to convert energy from waves is a challenge for the engineering community. The response of a wave energy device is generally frequency dependent, i.e. the resonance frequency and the frequency range which will give a significant response, will depend on the design of the device. A device will be exposed to a wide range of sea states characterized by the significant wave height H_s and a characteristic wave period, i.e. the spectral peak period T_p or the mean zero-crossing wave period T_z. Moreover, within a sea state, the individual random waves are characterized by the wave height H and the wave period T.

Knowledge of the statistical properties of the waves is crucial for designing a proper wave power device, i.e. both for the sea state and the single random waves within a sea state. It is also of interest to know e.g. the joint statistical properties of the wave power in a sea state with significant wave height or a characteristic wave period, or the joint statistics of the wave power for individual waves with the individual wave height or the individual wave period.

The purpose of this study is to discuss the long-term wave power statistics for individual waves and the power absorption for energy converters.

The student shall:

1. Give a background for long-term statistics, and discuss the long-term wave power statistics for individual waves by combining the short-term wave power statistics for individual waves in Myrhaug, Leira, Holm (2009) and the wave power statistics for sea states in Myrhaug, Leira, Holm (2011).
2. Give a review of control systems and power absorption.
3. Discuss the wave power absorption for energy converters as functions of significant wave height H_s and spectral peak period T_p.
4. Compute the long-term efficiency by using scatter diagrams of H_s and T_p.

In the thesis the candidate shall present his personal contribution to the resolution of problem within the scope of the thesis work.

NTNU Trondheim
Norwegian University of Science and Technology
Department of Marine Technology

Theories and conclusions should be based on mathematical derivations and/or logic reasoning identifying the various steps in the deduction.

The candidate should utilize the existing possibilities for obtaining relevant literature.

The thesis should be organized in a rational manner to give a clear exposition of results, assessments, and conclusions. The text should be brief and to the point, with a clear language. Telegraphic language should be avoided.

The thesis shall contain the following elements: A text defining the scope, preface, list of contents, summary, main body of thesis, conclusions with recommendations for further work, list of symbols and acronyms, reference and (optional) appendices. All figures, tables and equations shall be numerated.

The supervisor may require that the candidate, in an early stage of the work, present a written plan for the completion of the work. The plan should include a budget for the use of computer and laboratory resources that will be charged to the department. Overruns shall be reported to the supervisor.

The original contribution of the candidate and material taken from other sources shall be clearly defined. Work from other sources shall be properly referenced using an acknowledged referencing system.

The thesis shall be submitted in two copies:

- Signed by the candidate
- The text defining the scope included
- In bound volume(s)
- Drawings and/or computer prints that cannot be bound should be organized in a separate folder.
- The bound volume shall be accompanied by a CD or DVD containing the written thesis in Word or PDF format. In case computer programs have been made as part of the thesis work, the source code shall be included. In case of experimental work, the experimental results shall be included in a suitable electronic format.

Advisors : Professor Bernt J. Leira
Professor Dag Myrhaug

Deadline : 10.06.2012

Dag Myrhaug
Supervisor

Preface

This master thesis has been written at Department of Marine Technology, during the spring 2012 by Børge Sveaas Skøyen.

The topic of the project was chosen because it seemed interesting, and because I always have thought it was strange that wave energy isn't used for energy extraction all over the world, when the potential is so obvious. The scope of the project has been suggested by Professor Myrhaug and Professor Leira.

The main content of the project was to investigate long-term wave power statistics based on individual waves, look at some control systems for optimizing of WEC's and compare different WEC's efficiency in a long-term perspective. This has given me valuable knowledge, and has also increased my interest for wave energy as a field of study.

I wish to extend my thanks to my supervisors, Professor Dag Myrhaug and Professor Bernt J. Leira for helping, guiding and showing interest in my work.

Trondheim, 10. June 2012

Børge Sveaas Skøyen

Sammendrag

Langtidsstatistikk for bølgekraft beskriver forekomsten av bølger over år og deres energi. Dette blir funnet ved å sette sammen korttidsstatistikk for individuelle bølger og statistikk for sjøtilstander. Alle beregningene er gjort både ved bruk av bølgescatter diagrammer og analytiske uttrykk. De to uttrykkene gir jevnt over ganske like resultater.

For langtidsstatistikk er kvaliteten av resultatene avhengig av både oppløsningen på beregningene og størrelsen av området som beregningene spenner over. De fleste av bølgene har lave verdier for bølgeenergi, bølgehøyde og bølgeperiode. Det er sett at bølgekraft varierer med kvadratet av bølgehøyden, noe som er forventet. Langtids marginal pdf av bølgekraft er svært bratt og ligner en eksponentiell kurve, men den er ikke helt lik. CDF av bølgeenergi er også svært bratt, og her blir forskjellene mellom de to utregningsmetodene synlige.

For å optimalisere bevegelsene til en WEC i bølger er det nødvendig med et kontroll system. Målet med dette er å endre WEC-parametere slik at det øker bevegelse av de bevegelige delene. Den viktigste kontroll variabelen, maskineri kraften, kan deles i tre kategorier: resistiv last, reaktive last og ikke-lineær last. Ulike konsepter som bruker reaktiv last er omtrentlig kompleks konjugert kontroll, sporing av omtrentlig optimal hastighet og modell prediktiv kontroll. Disse gir den høyeste effekten, men de bruker litt energi for å kontrollere bevegelse. Disse metodene bruker en form for prediksjon fordi maskineristyrken er avhengig av fremtidige verdier. Resistiv belastning, dvs. ingen maskinkraft, blir presentert av fase kontroll ved hjelp av latching og clutching. Latching er en metode for å holde WEC'en fast i deler av syklusen, og clutching er en metode som omfatter kobling og frakobling av maskineriet i intervaller. Disse metodene gir mindre energiproduksjon, men de bruker ikke energi for å kontrollere fasen.

En god bølgeenergi konverterer er en enhet som har lave kostnader for elektrisitet per kilowatt time. Dette kriteriet er avhengig av prisen på enheten, som generelt er ukjent, og mengden absorbert kraft, som kan beregnes. Den absorberte kraften er beregnet for fire forskjellige konsepter: en bøye utsatt for hivbevegelse, en todelers enhet utsatt for hivbevegelse, en enhet med stamp bevegelse og en flytende OWC. Energiabsorberingen varierer for ulike sjøtilstander og øker generelt med bølgeenergien, men WEC'ene har ulike optimale verdier som gir best energiabsorpsjon og best effektivitet. Effektiviteten kan for enkelte områder være svært store, til og med større enn 100 % hovedsakelig på grunn av fokuserings teknikker og begrenset nøyaktighet på rådata som er benyttet i beregningene. Men de fleste av effektivitetsresultatene er mye lavere enn det. Effektiviteten av WEC'ene har blitt kombinert med langtids bølgekraftstatistikk for å komme fram til langtids energiabsorpsjon. Forskjellene mellom konseptene her er store, de har effektiviteter mellom 11% og 47%.

Summary

Long-term statistics for wave power describes the waves that will occur over years and their energy. This can be found by putting together short-term statistics for individual waves and statistics from sea states. All the calculations are done both by the use of wave scatter diagrams and analytical expressions. It is generally seen that the two different methods gives similar results.

For the long-term statistics the quality of the results is dependent on both the resolution of the calculations, and the size of which the calculations span over. Most of the waves have low values for wave energy, wave height and wave period. It is seen that the wave power varies with the square of the wave height which is expected. The long-term marginal pdf of wave power is very steep and resembles an exponential curve, but it is not an exact match. The CDF of wave energy is also very steep, and here the differences between the two methods become visible.

To optimize the motion of a WEC in waves a control system is necessary. The goal of the control system is to change the WEC's parameters so that it increases the motion of the moving parts. The key control variable, the machinery force, can be divided in three categories: resistive loading, reactive loading and non-linear loading. Different concepts that uses reactive loading is approximate complex conjugate control, tracking of approximate optimal velocity and model predictive control. These give the highest power output, but they use some energy in order to control the motion. These methods use prediction because the machinery force is dependent on future values. Resistive loading, i.e. no machinery force, is presented by phase control by latching and clutching. Latching is a method keeping the absorber fixed during parts of the cycle, and clutching is a method which is coupling and decoupling the machinery at intervals. These methods give smaller energy output, but do not use energy in order to control the phase.

A good wave energy converter is a device that has low cost of electricity per kilowatt hour. This criterion is dependent on the cost of the device, which is generally not known, and the power absorption that can be estimated. The power absorption has been estimated for four different concepts: a heaving buoy, a heaving two bodies system, a pitching device and a floating OWC. The power absorption varies for different sea states and is generally increasing as the total present wave power increases, but the WEC's have different optimal values that give the best power absorption and best efficiency. The efficiency can for some areas be very large, even larger than 100% mainly because of focusing techniques and limited accuracy on the raw data used in the calculations. However most of the efficiency results are much lower than that. The efficiency of the WEC's is combined with the long-term wave power statistics to obtain long-term power absorption. The differences between the concepts are large, as they have efficiency between 11% and 47%.

Contents

List of Figures

List of Tables

Nomenclature

Abbreviations

ACC	Approximate complex-conjugate control
AVT	Approximate optimal velocity
cdf	cumulative distribution function
MPC	Model-predictive control
OWC	Oscillating water column
pdf	probability density function
PMC	Peak-matching clutching control
PML	Peak-matching latching control
RL	Resistive loading
rms	root mean square
TUC	Threshold unclutching control
TUL	Threshold unlatching control
WEC	Wave energy converter

Greek letters

α	Weibull parameter
β	Weibull parameter
Δh	Interval size of h
ΔH_s	Interval size of H_s
Δj	Interval size of j

Δt	Interval size of t
ΔT_p	Interval size of T_p
η_{fowc}	Efficiency of the floating OWC
η_{H_s,T_p}	Efficiency of a WEC for a given sea state
η_{hb}	Efficiency of the heaving buoy
η_{htbs}	Efficiency of the heaving two-bodies system
η_{pd}	Efficiency of the pitching device
γ	Density of water $[kg/m^3]$
κ^2	Variance of lnH_s
λ	Wave length
μ	Mean value of lnT_p
ν	Shape parameter
ρ	Weibull parameter
σ^2	Variance of lnT_p
θ	Mean value of lnH_s
$\tilde{\beta}$	Weibull parameter
ζ	Weibull parameter
N_B	Total number of sea states

Roman letters

$\hat{J}$	Value for wich J shall not exceed in cdf
$\overline{T_z}$	Average mean zero crossing period
B_{H_s,T_p}	Number of sea states in a H_s and T_p-interval
b_{jh}	Number of waves in a j and h-interval
b_{jt}	Number of waves in a j and t-interval
d_a	Absorption width
$f(J)$	Long-term estimate of wave power
$F_J(\hat{J})$	Long-term cdf of wave energy
$f_{NB}(j \mid S)$	Narrow banded pdf of dimensionless wave energy given the sea state

$f_{NB}(J \mid S_i)$	Narrow banded pdf of wave energy given the sea state
$F_r(S_i)$	Probability of occurrence for a sea state
g	Gravitational acceleration $[m/s^2]$
H	Wave height $[m]$
h	Dimensionless wave height
H_{rms}	Root mean square-value of the wave height $[m]$
H_s	Significant wave height $[m]$
J	wave energy $[W]$
j	Dimensionless wave energy
J_{char}	Characteristic wave energy $[W]$
k	Shape parameter
N_b	Total number of individual waves in the scatter diagram
$p(h)$	Marginal pdf of h
$p(H_s)$	Marginal pdf of H_s
$p(H_s, T_p)$	Joint pdf of H_s and T_p
$p(j \mid h)$	Conditional pdf of j given h
$p(J, H \mid H_s, T_p)$	Joint pdf of wave energy and H
$p(j, h)$	Joint pdf of wave power and wave height
$p(J, T \mid H_s, T_p)$	Joint pdf of wave energy and T
$p(j, t)$	Joint pdf of wave power and wave period
$p(j; t)$	pdf of j, dependent on t
$p(t \mid j)$	Conditional pdf of t given j
$p(T_p \mid H_s)$	Conditional pdf of T_p given H_s
$p_{L,\eta}(J)$	Long-term marginal pdf of wave power absorption
$p_{L,\eta}(J, X)$	Long-term joint pdf of power absorption and either wave height or wave period
$p_L(H)$	Long-term marginal pdf of wave height
$p_L(J)$	Long-term marginal pdf of wave power

$p_L(J, X)$	Long-term joint pdf of J and X
$p_L(T)$	Long-term marginal pdf of wave period
S	A given sea state
T	Wave period $[s]$
t	Dimensionless wave period
T_j	Wave energy period
T_p	Spectral peak period $[s]$
T_{rms}	Root mean square-value of the wave period $[s]$
T_z	Mean zero crossing wave period $[s]$
$w(H_s, T_z)$	Ratio between number of waves in a sea state and average number of waves in the sea state
X	Either wave power or wave height

Chapter 1

Introduction

As the sun heats up the planet, it induces movement in the air that subsequently moves the water in the large oceans in the world. This continuous process will build up the waves, and by that transfer energy from the sun and wind to the water. In physics it is known that this transition will lead to an energy loss, and therefore the total wave energy capacity is less than the capacity for wind and solar energy. But the conversion will also increase the power density, and greater forces will occur in water than from wind or the sun. This energy can be exploited by converting it to useful energy that can be stored. This is done by devices that use the energy and movement in the waves to move pumps and turbines or other mechanisms, to transfer the energy. Thus they go by the name wave energy converters (WEC's).

For designing a WEC in the sea, the type of waves that it is exposed to is very important to take into account. The types of waves vary in a wide range of wave height and period and are affected by many parameters such as weather, season, wind and geographical location. Because of that the WEC cannot be designed for one specific wave. It has to be optimized to the wide range of waves present at an area. In order to do that, knowledge of both short-term statistics, describing variations within an individual sea state, and long-term statistics, describing variations over many sea states during many years, is necessary.

In order to optimize a WEC for a wide range of waves, the properties for specific waves have to be known. This introduces the need for short-term statistics. These statistics will give information for each single wave, and will therefore describe what a WEC experiences and gives as a power output when one wave passes by. And the power extracted is taken from each single wave passing by, and not an average value.

On the other hand the WEC are exposed to a wide range of waves over a lifetime,

and needs to be versatile to exploit the total potential in the waves. In order to take the lifetime into account and compare the total amount of extracted energy, long-term statistics is needed. Long-term statistics describes results over a longer period, and will include the results for a wide range of waves, thus describing the reality in a more complete way and give favourable results for concepts that can keep a high efficiency in a range of different wave heights and periods.

In order to get a best possible long-term description of the waves it should not only be made out of known sea states, put also for known individual waves. To obtain a perfect long-term distribution of waves individual waves have to be measured over a very long period. This is in most practical situations not doable. A way of solving this is to find a set of individual waves made dimensionless for the sea state they are collected in, and use them for every sea state that occur, to make a long-term statistics of the waves.

In the following text both equations for short-term statistics for individual waves and statistics for sea states shall be presented in order to find equations for long-term statistics for wave energy. Further the text shall look at control systems of WEC's that will increase the power absorption and efficiency by exploiting more of the potential in the waves. And finally the power absorption for some specific WEC concepts is presented and their efficiency in a long-term perspective is found. All the calculations are done in the matlab-program that is attached in appendix B.

Chapter 2

Background for Long-term statistics

In this chapter the background for what shall be used to find the long-term statistics is presented.

2.1 Basic equations

First some basic equations need to be presented in order to do the following calculations. These are commonly used formulas presented in many publications, for example by Myrhaug et al. [9]. The power in a wave is given as the transport of wave energy per unit crest length. For deep water this gives

$$J = \frac{\gamma g^2}{32\pi} H^2 T \tag{2.1}$$

where $\gamma = 1025 kg/m^3$ is the density of water, $g = 9.81 m/s^2$ is the gravitational acceleration, H is the wave height and T is the wave period.

Sea states can be described by many different parameters. A common way of describing it is with significant wave height and mean zero crossing period or spectral peak period. Another way is by using the root mean square-value (rms), which is an average value for the sea state. The rms-value for the wave height has a relation to the significant wave height H_s given as

$$H_{rms} = 0.714 H_s \tag{2.2}$$

and the rms-value for the wave period has a relation to the mean zero crossing wave period T_z and the spectral peak period T_p given as

$$T_{rms} = 1.2416 T_z = 0.97 T_p \tag{2.3}$$

This fixed relationship between the mean zero crossing wave period and the spectral peak period is an approximation, and in reality this relationship will depend on the sea state.

2.2 Short-term wave power statistics for individual waves

In order to look at long-term statistics for individual waves, short-term statistics for individual waves are described first. This will in a later stage be used as a part of the calculations for the long-term statistics.

2.2.1 Dimensionless values

When looking at short-term statistics for individual waves it is preferable that they are independent from the sea state that they are measured in. This makes it possible to use the same individual waves for different sea states. The following formulas are also from Myrhaug et al. [9]. By dividing on the rms-value for the wave height and wave period, the values become dimensionless and independent on the sea state. Dimensionless wave height h is given by

$$h = \frac{H}{H_{rms}} \tag{2.4}$$

where H is the wave height in meters, and H_{rms} is the rms-value of the wave height from the sea state. Dimensionless wave period t is given by

$$t = \frac{T}{T_{rms}} \tag{2.5}$$

where T is the wave period in seconds, and T_{rms} is the rms-value of the wave period from the sea state. In order to get dimensionless wave energy a characteristic wave energy parameter is introduced given as

$$J_{char} = \frac{\gamma g^2}{32\pi} H_{rms}^2 T_{rms} \tag{2.6}$$

where γ is the density of water, g is the gravitational acceleration, H_{rms} is the rms wave height and T_{rms} is the rms wave period. This is used to get the dimensionless wave energy

$$j = \frac{J}{J_{char}} \tag{2.7}$$

By inserting equation 2.1, 2.4, 2.5 and 2.6 into 2.7, the dimensionless relationship between wave energy, wave height and wave period will be obtained as

$$j = h^2 t \tag{2.8}$$

This will connect each wave, with its wave height and wave period, to a wave power.

2.2.2 Using wave scatter diagram

To find the statistical properties of individual waves a wave scatter diagram can be used. The wave scatter diagram, given in appendix A.2, are made out of measurements at sea on the Norwegian continental shelf including 6353 individual zero-down cross waves. The data is sampled with three Waverider buoys in deep water. The scale of the wave height and period is made dimensionless by the rms-value as described in section 2.2.1.

2.2.3 Rearranging the scatter diagram

The wave scatter diagram shows all the waves in a table where they are placed in intervals based on the h (rows) and t (columns) values. However the main interest is to look at the wave energy. And as described the wave energy for dimensionless values is given by $j = h^2 t$. In this way all the waves that already have a h and t value gets a j value and the scatter diagram can be re-arranged to be sorted for j and h or j and t. This way of writing the scatter diagram is beneficial in a later stage.

To re-arrange the scatter diagram the j-values need to be divided in intervals of a suitable size. But it is difficult to find a size that does not introduce problems with the resulting wave scatter diagram. Because the resulting graphs are very steep at some areas it is preferable to keep the intervals small. But that will introduce some problems for some values. One thing is that the scatter diagram is put together by a finite number of waves, so if the intervals become too small there would not be enough waves to fill the intervals. Another similar example of Δj not being large enough is for larger values of both j and t, when the jumps of the values for h^2t is larger than Δj. If $\Delta j = 0.5$ this will occur for the intervals $t = 0.85$ and $j = 2.75$ which will include values between $j = 2.5$ and $j = 3.0$. The possible outcome of j-values will jump from 2.45 to 3.06 because of j being a function of h. In other words, there will be some places in the scatter diagram where there is no possibility for a wave to occur even though it is many waves in that area, and this will be problematic and lead to errors. Another problem with making new scatter diagrams varying with j is that these scatter diagrams are supposed to be used for different sea states. That means that sea state parameters like H_{rms} and T_{rms} have to be included, introducing dimensions again. This again will change the interval sizes based on the sea state, and make unique scatter diagrams for each sea state. So it has to be created as many scatter diagrams as there are sea states which seem unnecessary.

These problems have been solved by distributing all the waves in each interval over the area of the interval. In other words, each wave gets individual values for wave height and period. Ideally each wave should have its unique value for h and t measured from real life, but in the scatter diagram the waves are added up in discrete values of a given interval size. By assuming that all the waves are distributed and have exact values for h and t, each wave can easily be put inside different intervals at a later stage, and the problem is solved.

The goal of how the waves are distributed is to evenly place each wave over the whole interval, but because the numbers seldom adds up to a square it has to be solved a little differently. The method that is used is taking the square root of the wave number in the interval and round it down to the closest integer. This integer is the number of waves in each direction, and they are uniformly distributed. The remaining waves are again taken the square root of, and the procedure is repeated until there are no more waves. How the different waves are distributed is figuratively described in figure 2.1.

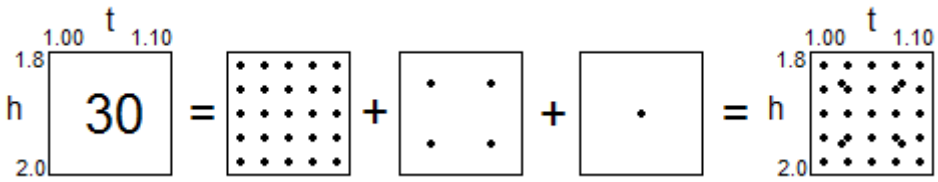

Figure 2.1: How the waves in the scatter diagram is distributed. The figure shows an example of an interval containing 30 waves.

This would simulate how waves are in reality, but with some problems. The assumption that all the waves should be evenly distributed is not perfect. Ideally the data telling the wave height and period for each wave should have been known, and in order to simulate that, and get something similar to continuous wave measurements, it is assumed that they are evenly distributed. A improvement of that would maybe be to adjust the distribution to how many waves there are in the neighbouring h and t intervals, distribute them randomly, or in another way introducing a more complete distribution, but in this case a uniform distribution is assumed to be sufficient, and maybe also best suited when the goal is to fill up the intervals with j-values. The result of this is presented in figure 2.2.

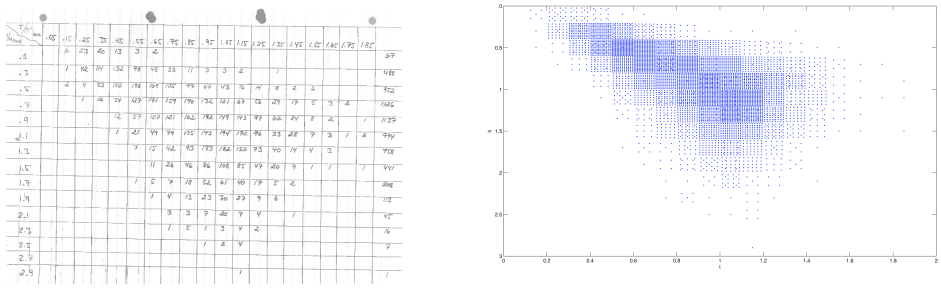

Figure 2.2: left: The original scatter diagram. right: The uniformly distributed scatter diagram.

2.2.4 Calculating the probabilities by scatter diagram

Then the probability of some event to occur can be calculated. This is easily done by taking the number of waves at a given interval and divide it on the total number of waves and the size of the interval. This gives the equations

$$p(j,h) = \frac{b_{jh}}{N_b \Delta j \Delta h} \tag{2.9}$$

where b_{jh} is the number of waves in the interval, N_b is the total number of individual waves, and Δj and Δh is the size of the interval, and

$$p(j,t) = \frac{b_{jt}}{N_b \Delta j \Delta t} \tag{2.10}$$

where b_{jt} is the number of waves in the interval, N_b is the total number of individual waves, and Δj and Δt is the size of the interval.

2.2.5 Using analytical expressions

The probability distribution described by the scatter diagram can also be described by analytical expressions made of known distributions such as the Weibull distribution. This is done by Myrhaug et al. (2009) [9]. Here a joint probability density function (pdf) of h and t are used to provide the statistical properties of j. This distribution is based on the same wave scatter diagram which is described in section 2.2.2.

The joint pdf of wave power and wave height is given as

$$p(j,h) = p(j|h)p(h) \tag{2.11}$$

where the marginal pdf of h is given by the 2-parameter Weibull pdf

$$p(h) = \frac{2.39h^{1.39}}{1.05^{2.39}} exp\left[-\left(\frac{h}{1.05}\right)^{2.39}\right]; h \geq 0 \tag{2.12}$$

and the conditional pdf of j given h is given by the 3-parameter Weibull pdf

$$p(j|h) = \frac{\beta}{\rho h^2}\left(\frac{j-\alpha h^2}{\rho h^2}\right)^{\beta-1} exp\left[-\left(\frac{j-\alpha h^2}{\rho h^2}\right)^{\beta}\right]; j \geq \alpha h^2 \tag{2.13}$$

with the parameters

$$\alpha = 0.12\sqrt{h} \tag{2.14}$$

$$\rho = \begin{cases} 0.78h + 0.26 & ; h \leq 0.9 \\ 0.962 & ; h > 0.9 \end{cases} \tag{2.15}$$

$$\beta = 2arctg[2(h - 1.2)] + 5 \tag{2.16}$$

The joint pdf of wave power and wave period is given as

$$p(j,t) = p(t|j)p(j;t) \tag{2.17}$$

where the pdf of j, which is dependent on t, is given by the 2-parameter Weibull pdf

$$p(j;t) = \frac{s}{r}\left(\frac{j}{r}\right)^{s-1} exp\left[-\left(\frac{j}{r}\right)^{s}\right] \quad ; j \geq 0 \tag{2.18}$$

where

$$r = 1.05^2 t \tag{2.19}$$

$$s = 2.39/2 \tag{2.20}$$

and the conditional pdf of t given $h = \sqrt{j}/\sqrt{t}$ is given by the 3-parameter Weibull pdf

$$p(t|h = \frac{\sqrt{j}}{\sqrt{t}}) = \frac{\beta}{\rho}\left(\frac{t-\alpha}{\rho}\right)^{\beta-1} exp\left[-\left(\frac{t-\alpha}{\rho}\right)^{\beta}\right] \quad ; t \geq \alpha \tag{2.21}$$

where α, ρ and β is given in the equations 2.14, 2.15 and 2.16 by substituting for $h = \sqrt{j}/\sqrt{t}$.

2.2.6 Comparing analytical expressions and scatter diagram

Comparing the analytical formulas to the values in the wave scatter diagram is of interest because it would give an indication of how good the analytical expressions match the results from the scatter diagram that they are based on. The biggest difference between them is that the analytical expressions are made as a continuous function from the scatter diagram which is discrete. This could lead to some problems when comparing them. However it is important to acknowledge that the scatter diagram is not completely true either. The waves that are of continuous height and period in reality are simplified into discrete values, and then theoretically put back into "true" values by evenly distributing them as described in chapter 2.2.3.

One problem is the resolution of the calculations. For analytical expressions it is preferable to calculate values in very small intervals. An example of this being important is when both the wave power and the wave height is very small. Here the distribution curves are very steep, and if the intervals is not small enough the calculations will miss many of the maximum values. On the other hand there is the scatter diagram which have limitations of how small the intervals can be. The scatter diagram have a limited number of waves, and if they are distributed over a very large number of intervals the representation will become very fragmented, simply because there are not enough waves.

Another thing to think about is the total span of the calculations. It is preferable that integration over the total area sums up to the value of 1, but this would often need a very large area of calculations, where most of the parts is not very interesting. For discrete values this area is of a finite size and it can be tested if the value equals 1, but for the formulas the integration have to be done to infinity, so anything that is close to 1 would be satisfying. When presenting the results it would be better to find a size of the area that represents the total distribution well, but still is so small that the interesting parts is in focus.

2.2.7 Deviation between scatter diagram and analytical expressions

To compare the different curves a method for analysing the deviation between scatter diagram and analytical expressions have to be applied. This can be done in many different ways with both different complexity and different type of output. The most important is that the deviation can give an understandable value that somehow shows the actual magnitude of the deviation. These have been the main considerations when estimating the deviation and has led to the use of two different ways of presenting the deviation.

The first way of presenting the deviation is looking at the total integrated area of

the graph for the analytical expressions and the scatter diagram values. Because the values are probabilities it is obvious that the true value should be one, and the deviation from the true value is therefore easy to compare. However it doesn't say anything of where the deviation occur, and even though the total difference might be very small, there still can be large local differences, which for the whole set evens out.

To find the location of the deviation a second method is introduced. The second method to present the deviation is a plot that shows the local deviation for each point value. The deviation is given by taking the square of the difference between the analytical value and the scatter diagram value. Therefore it is quite difficult to actually imagine the magnitude of the deviation. But it gives a great overview of where the largest differences occur. A problem with this method is that the point value is taken at values matching the discrete intervals for the analytical solution. This is a bit course for the analytical formulas and may give errors where the curves are steep.

Together these two methods can give a good total impression of the deviation because they as a whole fulfill the need for estimating the deviation.

2.2.8 Results

When looking at table 2.1 the integrated total area of the graph for different plots are presented. As they are probabilities the area preferably should be 1. But because this is not exact calculations anything close to 1 is satisfying. For the scatter diagram values the number is decided based on how many of the waves from the scatter diagram that are included in the calculations. So they will be 1 when the area covered is as large as the scatter diagram. When taking a smaller area some of the extreme waves will disappear, but the number is still close to 1. When looking at analytical values it is seen that the number is mostly based on the resolution of the calculation. This is because if the resolution is to low the calculations will miss out on peaks and give a too low value. It is also interesting to see that the formula values have almost the same reduction as the scatter diagram values when going from a large area to a small area.

Short-term	low res large	low res small	high res
Int. area of $p(j,h)$ from scatter diagram	1.0000	0.9830	0.9830
Int. area of $p(j,h)$ from formulas	0.8819	0.8665	0.9679
Int. area of $p(j,t)$ from scatter diagram	1.0000	0.9830	0.9830
Int. area of $p(j,t)$ from formulas	0.9918	0.9765	0.9849

Table 2.1: Integrated total area for different individual wave graphs with different sizes and resolutions

In the following calculations where the scatter diagram and formula values are compared they are plotted with the same size, so that they can be compared, but the resolution is higher for the plot from analytical expressions than for the plots form the wave scatter diagrams. In the plots it is not necessary to include the large area because the extreme values would not be visible. Preferably the high resolution calculations should be used also for the scatter diagram values, but a high resolution would be a problem because of the limited amount of waves. This will lead to a very fragmented picture. So therefore the low resolution are used in the plots.

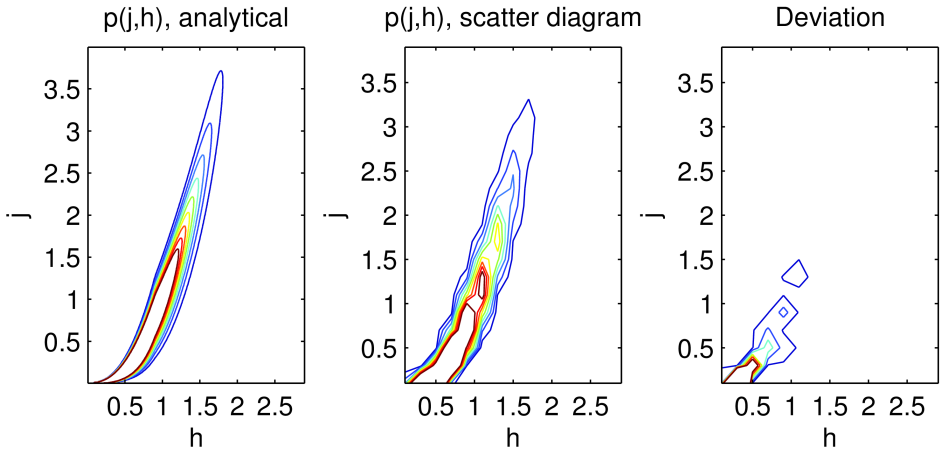

Figure 2.3: Plot of p(j,h) for analytical expressions, scatter diagram and the deviation. The levels of the outer contours are 0.1 0.2, 0.3, 0.4, 0.5, 0.6, 0.7, 0.8 and 0.9 for the two to the left. For the deviation the outer contours are 0.01, 0.1, 0.2, 0.3, 0.4 and 0.5.

In figure 2.3 the joint pdf of dimensionless wave power and wave height $p(j, h)$ is plotted. From the shape of the contours it is seen that the curves are very step, especially for low values. It is also seen that the shape fits with the fact that j increases with the square of h. It is seen that the values from the formulas and scatter diagram look quite similar. And from the deviation it is seen that the main part of the differences are for low values of h and j. This is where the curves are very steep, and the deviation could be expected to be of some size. When the total area of the graph is integrated the scatter diagram plot gives the value 1 as expected. In theory the formula plot should also give the value 1, but it gives the value 0.97. However it is seen that it would go to 1 as the interval sizes decreases.

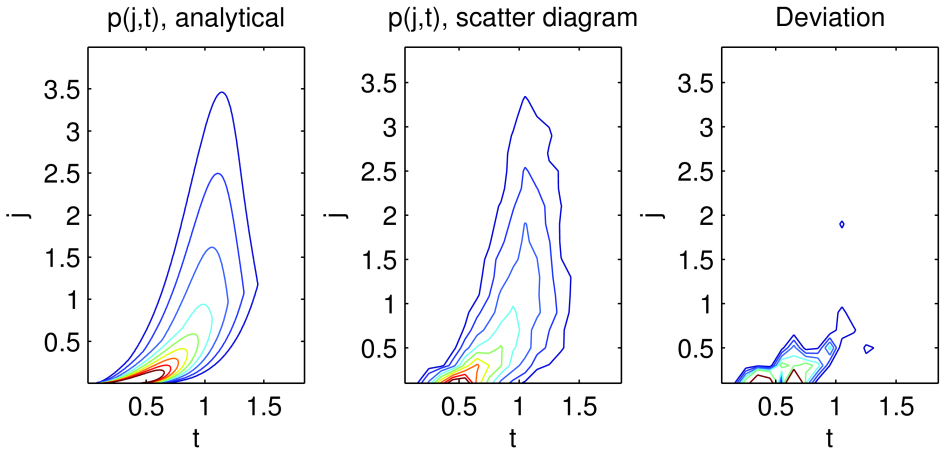

Figure 2.4: Plot of p(j,t) for analytical expressions, scatter diagram and the deviation. The levels of the outer contours are 0.1, 0.25, 0.5, 0.75, 1.0, 1.25, 1.5, 1.75 and 2.0 for the two to the left. For the deviation the outer contours are 0.01, 0.02, 0.03, 0.04, 0.05 and 0.1.

In figure 2.4 the joint pdf of wave power and wave period $p(j,t)$ is plotted. The shape of the plot is not as steep as in figure 2.3, except at the peak. It seems that the fit between the scatter diagram values and the analytical values is good. Most of the deviation are located for small values of j where the curves are steep. For integration of the total area of the graph the scatter diagram gives the value of 1 and the formula gives the value of 0.99. Also here it is seen that decreasing interval size is necessary to get a satisfying result, but it is not as sensitive for larger intervals as $p(j,h)$.

2.3 Wave statistics for sea states

In long-term statistics also statistics for which sea states that occur is necessary. This will be described here, and in a later stage be used as a part of the calculations for the long-term statistics.

2.3.1 Using wave scatter diagram for sea states

The sea state scatter diagram, given in appendix A.1, are made out measurements from Haltenbanken between 1980 and 1985. When using this scatter diagram there is no need to rearrange it similarly as was done for the individual waves scatter

diagram. This is because the original form is used as it is in a later stage. The only change that is done is that the end intervals for this scatter diagram is changed in order to be able to do the calculations. In the scatter diagram this is done in such way that they sum up all the waves less than or larger than a value, thus the interval size will be of larger size than all the others. This is changed so that they are assumed to have the same interval size as the other intervals, and values less than this interval is neglected because they are assumed to not have any waves.

2.3.2 Calculating the probabilities from scatter diagram

The probability is found directly by taking the number of waves in an interval and divide it on the total number of waves in the scatter diagram and the interval size. The joint pdf of H_s and T_p is given as

$$p(H_s, T_p) = \frac{B_{H_s,T_p}}{N_B \Delta H_s \Delta T_p} \tag{2.22}$$

where B_{H_s,T_p} is the number of sea states in the interval, N_B is the total number of sea states, and ΔH_s and ΔT_p is the size of the interval.

2.3.3 Using analytical expressions

Similarly as for the individual waves, the sea states can also be described as analytical expressions. This is done by Myrhaug et al. (2011) [7]. The joint pdf of H_s and T_p is given as

$$p(H_s, T_p) = p(T_p \mid H_s) p(H_s) \tag{2.23}$$

where the marginal pdf of H_s is given as

$$p(H_s) = \begin{cases} \frac{1}{\sqrt{2\pi}\kappa H_s} exp\left[-\frac{(\ln H_s - \theta)^2}{2\kappa^2}\right] & ; H_s \leq 3.25m \\ \tilde{\beta}\frac{H_s^{\tilde{\beta}-1}}{\zeta^{\tilde{\beta}}} exp\left[-\left(\frac{H_s}{\zeta}\right)^{\tilde{\beta}}\right] & ; H_s > 3.25m \end{cases} \tag{2.24}$$

with the mean value $\theta = 0.801$, variance $\kappa^2 = 0.371$ of lnH_s, and the Weibull parameters $\zeta = 2.713$ and $\tilde{\beta} = 1.531$. The conditional pdf of T_p given H_s is given by

$$p(T_p \mid H_s) = \frac{1}{\sqrt{2\pi}\sigma T_p} exp\left[-\frac{(\ln T_p - \mu)^2}{2\sigma^2}\right] \tag{2.25}$$

with the parameters

$$\mu = a_1 + a_2 H_s^{a_3} \quad ; (a_1, a_2, a_3) = (1.780, 0.288, 0.474) \tag{2.26}$$

$$\sigma^2 = b_1 + b_2 e^{b_3 H_s} \quad ; (b_1, b_2, b_3) = (0.001, 0.097, -0.255) \tag{2.27}$$

2.3.4 Results

In figure 2.5 the joint pdf of significant wave height and spectral peak period $p(h_s, T_p)$ is plotted. It distributes revolving the peak at $H_s = 2m$ and $T_p = 8s$. Contrary to the scatter diagram for the individual waves, this scatter diagram is not rewritten to vary with j, thus it would be expected that the local deviation is small. For the integrated total area of the graph the scatter diagram gives the value of 1 and the formula gives the value of 0.999. It can also be seen on the magnitude of the contour lines of the deviation compared to the contour lines of the distribution that the deviation is small. For these calculations the area of the size of the scatter diagram is used as it gives satisfying results, and the resolution is similar to the scatter diagram.

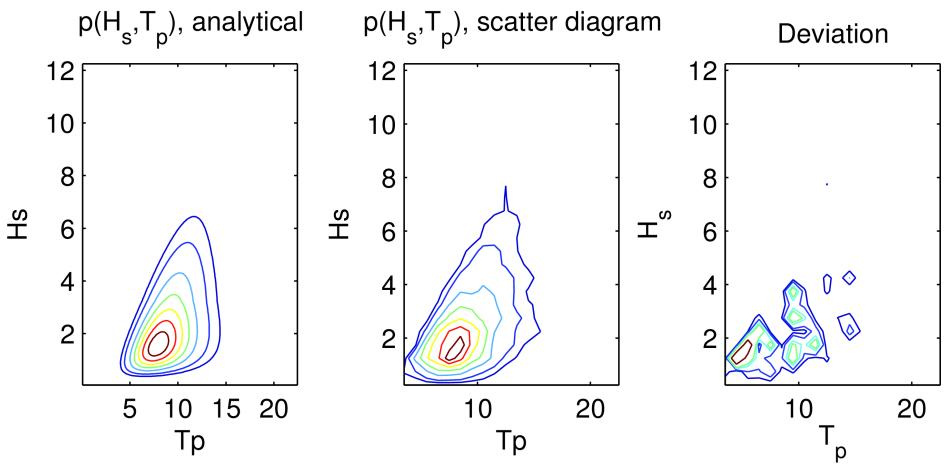

Figure 2.5: Plot of $p(h_s, T_p)$ from analytical expressions, scatter diagram and the deviation. The levels of the outer contours are 0.005, 0.01, 0.02, 0.03, 0.04, 0.05 and 0.06 for the two to the left. For the deviation distribution the outer contours are 0.00001, 0.00002, 0.00004, 0.00005 and 0.0001.

Chapter 3

Long-term wave power statistics

Long-term wave power statistics describes the variations in wave power over a long-term collection of sea states, for example with the duration of 20 years. This can be used for finding the extracted wave power for a WEC in a lifetime, and it will describe which waves giving the largest contribution.

3.1 Simplified long-term distribution

One way of finding the long-term wave power statistics is the way presented by Izadparast and Niedzwecki [5]. By assuming that the waves have a narrow-banded energy spectrum, the probability distribution for the waves in a given sea state would follow an exponential distribution. So the narrow banded probability distribution would be

$$f_{NB}(j \mid S) = exp(-j) \tag{3.1}$$

where j is the dimensionless wave power and S is the given sea state. From that the long-term estimate is obtained from the summation taken over all the possible sea states of the product obtained from multiplying the mean wave power with the long-term averaged probability of occurrence of the corresponding sea state,

$$f_{NB}(J) = \sum_i f_{NB}(J \mid S_i) F_r(S_i) \tag{3.2}$$

where J is the wave power with dimensions, S_i is the sea state together giving the probability density function for the wave power for a given sea state $f_{NB}(J \mid S_i)$ and $F_r(S_i)$ is the probability of occurrence for the sea state. This will suggest exponential behaviour of the long-term distribution

This method introduces the basic thoughts of how to find long-term statistics. However it is a simplified representation of how to find it. For example waves in the ocean is not narrow banded which is assumed by this approach, and this does not take individual waves into account.

3.2 Long-term distribution based on individual waves

Another way of finding long-term statistics is to use a method closer to the reality and by not doing the simplifications described in section 3.1, is done by Myrhaug et al. [8]. Here the long-term statistics is derived by combining the statistics for individual waves and sea states. This is done with a large amount of real waves and will therefore be more certain to describe a correct long-term distribution of wave power. The problem with this approach is that it will lead to a larger equation which demands more computation time, and it also needs more information.

The long-term joint pdfs of wave power and wave height and for wave power and wave period are obtained by integration of the joint pdf of wave energy and either wave height or wave period over the significant wave height and spectral peak period, both given by the sea state. This gives the equation

$$p_L(J, X) = \int_0^\infty \int_0^\infty p(J, X \mid H_s, T_p) p(H_s, T_p) w(H_s, T_z) \mathrm{d}H_s \mathrm{d}T_p \tag{3.3}$$

where $p(J, X \mid H_s, T_p)$ is the joint pdf of wave energy and either wave height or wave period for a given sea state, $p(H_s, T_p)$ is the joint pdf of the significant wave height and the spectral peak period given in equation 2.23, and $w(H_s, T_z)$ is the ratio between the number of waves in a sea state and the average number of waves in the sea states.

The joint pdf of wave energy and either wave height or wave period for a given sea state is found by using the Jacobian $|\partial j/\partial J, \partial h/\partial H|$ and $|\partial j/\partial J, \partial t/\partial T|$, to get

$$p(J, H \mid H_s, T_p) = \frac{p(j,h)}{J_{char} \times H_{rms}} \tag{3.4}$$

and

$$p(J, T \mid H_s, T_p) = \frac{p(j,t)}{J_{char} \times T_{rms}} \tag{3.5}$$

where $p(j,h)$ is given in equation 2.11 and $p(j,t)$ is given in equation 2.17. The ratio between the number of waves in a sea state and the average number of waves in the sea states can be given as

$$w(H_s, T_z) = \frac{\overline{T_z}}{T_z} \tag{3.6}$$

where $\overline{T_z}$ is the average mean zero crossing period of all the sea states and T_z is the mean zero-crossing wave period. This average mean zero crossing period can be found by the equation

$$\overline{T_z} = \int_0^\infty exp(\mu + \frac{1}{2}\sigma^2) p(H_s) \mathrm{d}H_s \tag{3.7}$$

where μ is given in equation 2.26 and σ is given in equation 2.27.

3.2.1 Using scatter diagram on the long-term statistics

Instead of using analytical expressions, scatter diagrams for the waves can be used to calculate the probability distributions. The use of scatter diagrams will give discrete values and equation 3.3 have to be changed into

$$p_L(J, X) = \sum_{i=1}^{\infty} \sum_{j=1}^{\infty} p(J, X \mid H_{s,i}, T_{p,j}) p(H_{s,i}, T_{p,j}) w(H_{s,i}, T_{z,j}) \Delta H_s \Delta T_p \tag{3.8}$$

where the different parts have the same meaning as before. All of these probabilities are given by the use of scatter diagrams. The joint pdf of wave energy and either wave height or wave period for a given sea state with a specified significant wave

height and spectral peak period is found by combining equation 2.11 and 3.4, and equation 2.17 and 3.5 to

$$p(J, H \mid H_s, T_p) = \frac{b_{jh}}{N_b \Delta H_s \Delta T_p} \tag{3.9}$$

$$p(J, T \mid H_s, T_p) = \frac{b_{jt}}{N_b \Delta H_s \Delta T_p} \tag{3.10}$$

where b_{jh} and b_{jt} is the number of waves in the interval, N_b is the total number of individual waves, and ΔH_s and ΔT_p is the size of the interval. The expressions for the joint pdf of the significant wave height and the spectral peak period is given in equation 2.22. $w(H_s, T_z)$ is the ratio between the number of waves in a given sea state and the average number of waves in all the sea states. Because the same scatter diagram for individual waves is used for every sea state, all the sea states have the same number of waves, so

$$w(H_{si}, T_{zj}) = 1 \tag{3.11}$$

3.3 Results for long-term statistics

Before the calculations can start some decisions need to be done. The size of the plotted area have to be decided based on which J-values and H- and T-values occurs. And the resolution of the calculations have to be decided based on how small intervals that is necessary to represent the equations properly. Another thing that has been done is that the wave energy is changed from Watt to Mega Watt. This means that the interval size of the wave energy will become in the size range of 10^0 instead of 10^6, and that the pdf-values in the graphs is in the size range of 10^0 instead of 10^{-6}. This will make the numbers a bit easier to understand.

3.3.1 Size of the calculations

In order to decide the size of the plotted area it is made a simple figure which spans over a large area, including all the waves from the scatter diagram, showing how they are distributed. This is given in figure 3.1. As can be seen, if all the waves are to be included the calculations have to span over a rather large area with values up to wave power of $12MW$, wave height up to almost $30m$ and wave period up to $40s$. However there are very few waves that have such large values, so those parts are not very interesting to include.

The yellow part in the graph includes values up to wave power around $3MW$, wave height up to $15m$ and wave period up to $30s$. This includes 99.9% of the waves, and would be better choice than the eight times larger alternative which includes all the waves.

The red part in the graph only includes very low values of wave power, wave height and wave period, but it still includes 94.5% and 92.9% of the waves. However the problem with these waves are that most of them contains very little energy, and by only looking at that part the waves with more energy are excluded. Also the pattern of how the waves are distributed will be interesting, and that will not be included in the red part of the graph.

Because this is probabilities the area under the curves should sum up to the value of 1. To get this the calculations have to include all the waves, and because some waves represents rather extreme values this means that the calculations have to span over large areas. However most of the waves are located in a much more limited area, which is the area of interest. So it is better to concentrate the plots on the areas with large probabilities even though it does not include all the waves. Therefore the plots are made with the goal of including most of the waves in a reasonable size, thus they are plotted over the yellow area.

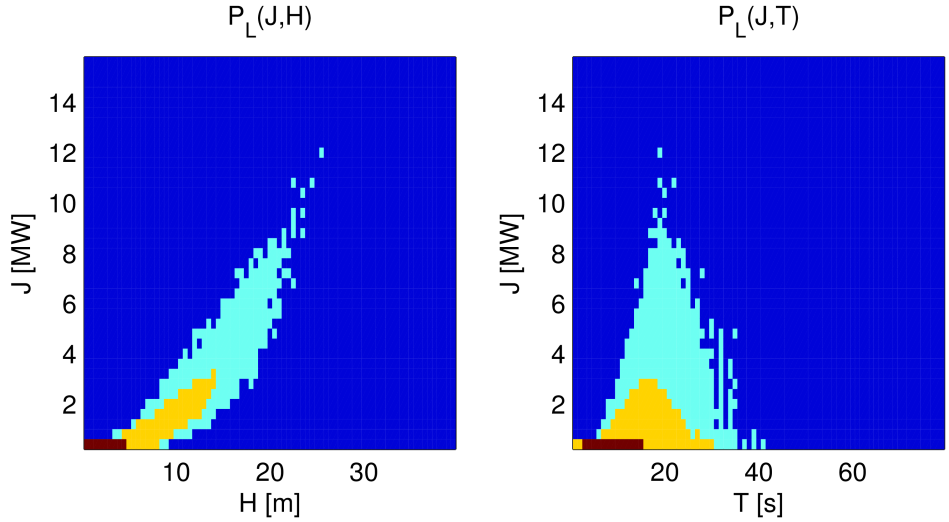

Figure 3.1: Plot showing long-term distribution of all the waves over a large span, where the cyan coloured part contains all of the waves, the yellow part contains 99.98% of the waves when plotted for H and 99.96% when plotted for T , and the red part contains 94.47% of the waves when plotted for H and 92.86% when plotted for T .

3.3.2 Resolution of the calculations

Before the calculations are done some tests of the resolution needs to be done. This is tested with a low resolution, and a high resolution that is ten times finer than the low resolution for both wave energy and wave height/period. The choice of resolutions are based the results from table 2.1.

Long-term	low res	high res
Integrated area of $p_L(J,H)$ from scatter diagram	0.9999	0.9999
Integrated area of $p_L(J,T)$ from scatter diagram	0.9999	0.9999
Integrated area of $p_L(J,H)$ from analytical expressions	0.4518	0.9505
Integrated area of $p_L(J,T)$ from analytical expressions	0.4517	0.9505
Computation time	31 min	2482 min

Table 3.1: Integrated total area for different long-term graphs for high and low resolution

In table 3.1 different values for the integrated total area of the graph are presented for both high and low resolution calculation. For the scatter diagram values it is seen that it gives very good results for both low and high resolution, but the problem is that for high resolution the plots gets very fragmented because of the limited number of waves. For the analytical calculations the difference between high and low resolution is very large. For the low resolution the integrated total area is only 45%. This is very low, and is not acceptable. It is however seen that most of the missing volume is for very low values of J and that the analytical expressions gives satisfying results for high J-values, so the problem is mainly when the curves are steep. Because the intervals are too large they does not include the high concentration of waves that have very small values of J. When the resolution is increased the value become 95%, which is a more acceptable value. Then the intervals are small enough to include the waves with close to zero in wave energy. So to sum up the scatter diagram calculations need to have low resolution, so that they does not become too fragmented, and the formula calculations need to have high resolution, so that they include a large enough percentage.

Another thing to notice is the calculation time. In order to do the high resolution calculations the computer needs 2482 minutes (very slow computer), but for the low resolution calculations it only takes 31 minutes. This is very large difference, and it demands very much time to get a satisfying result for the analytical calculations.

3.3.3 Long-term pdf of wave energy

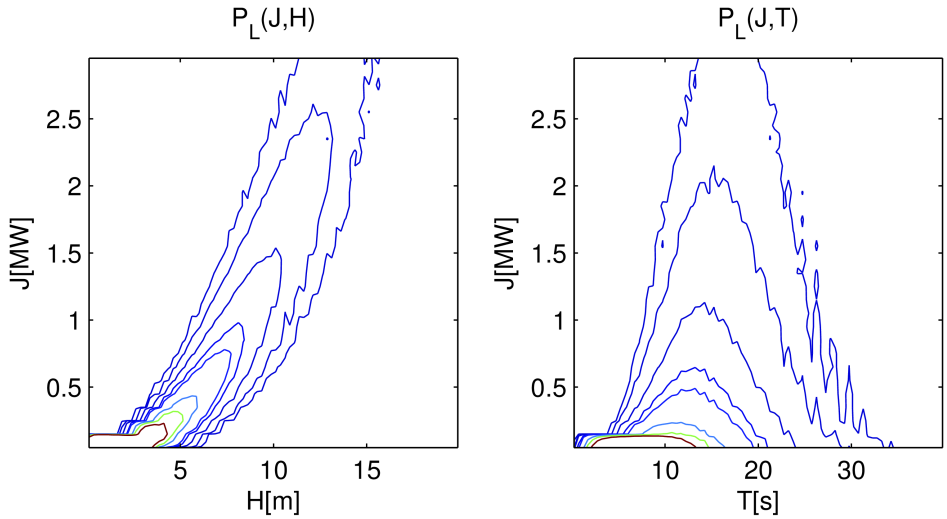

Figure 3.2: Plot showing $p_L(J, H)$ and $p_L(J, T)$ calculated from the scatter diagram, where the contours are 0.00001, 0.0001, 0.001, 0.005, 0.01, 0.05, 0.1 and 0.2.

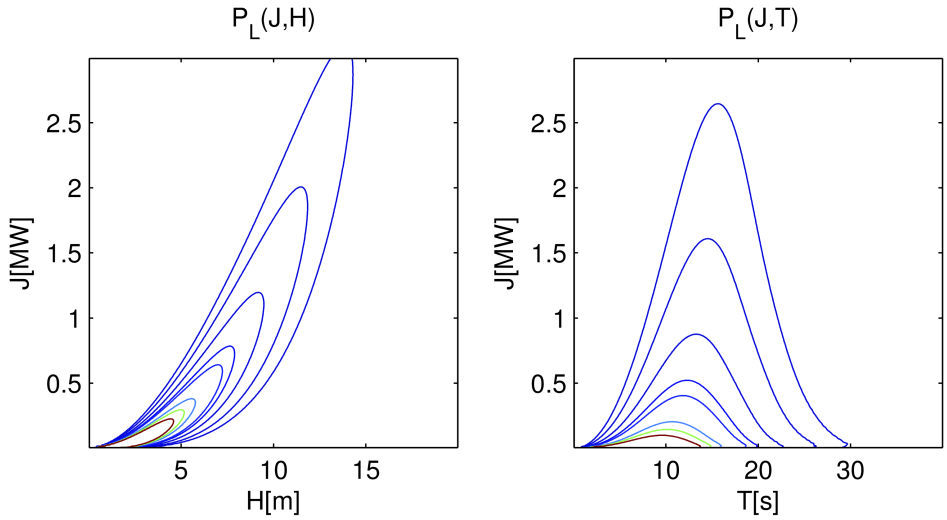

Figure 3.3: Plot showing $p_L(J, H)$ and $p_L(J, T)$ calculated from analytical expressions, where the contours are 0.00001, 0.0001, 0.001, 0.005, 0.01, 0.05, 0.1 and 0.2.

In figure 3.2 the probability distribution $p_L(J,H)$ and $p_L(J,T)$ from scatter diagram calculations are presented. In figure 3.3 the probability distribution $p_L(J,H)$ and $p_L(J,T)$ from formulas are presented. When comparing them it is seen that they have the same shape and varies similarly as the energy increases. It is seen that the formula plot gives better visualization at the small values for wave energy and wave height/period because of the limited resolution of the scatter diagram plots. The scatter diagram plots also gets a bit fragmented for large values, so the resolution could not be any higher. As all the plots are made with the same contours it is seen that the scatter diagram values are generally a bit higher than the formula values. This can easily be seen for the outermost contours. This is the consequence of the formula plot only covering 95% of the area that it is supposed to cover.

When looking at the trends in the plot it is seen that the most occurring waves are in areas of low energy, and the occurrence for waves with larger energy decreases rapidly. It is also seen on the plot for $p_L(J,H)$ that the wave energy increases with what looks like the square of the wave height, as would be expected by theory.

When comparing with the plots for the individual waves presented in figure 2.3 and 2.4, which shows dimensionless values where the sea state is isolated, it shows some similarities. The variation of the wave energy with wave height follows a similar shape and the variation of wave energy with waver period is only a bit different for large wave periods and small wave energy. However the largest difference for both is that the long-term distribution is much more concentrated around low wave energy, and are much steeper.

3.3.4 Long-term pdf of wave energy weighted for wave energy

The probability distribution of the waves are important information and very interesting, but it does not directly take into account the actual wave energy produced at given parameters. In order to find the energy output distribution the probability of a wave should be weighted for the wave power, by multiplying with the wave power. That will give a more interesting figure if the goal is to find out what kind of waves gives most energy over a long-term perspective. The values are multiplied with the wave energy in mega watt so that the same contours can be used.

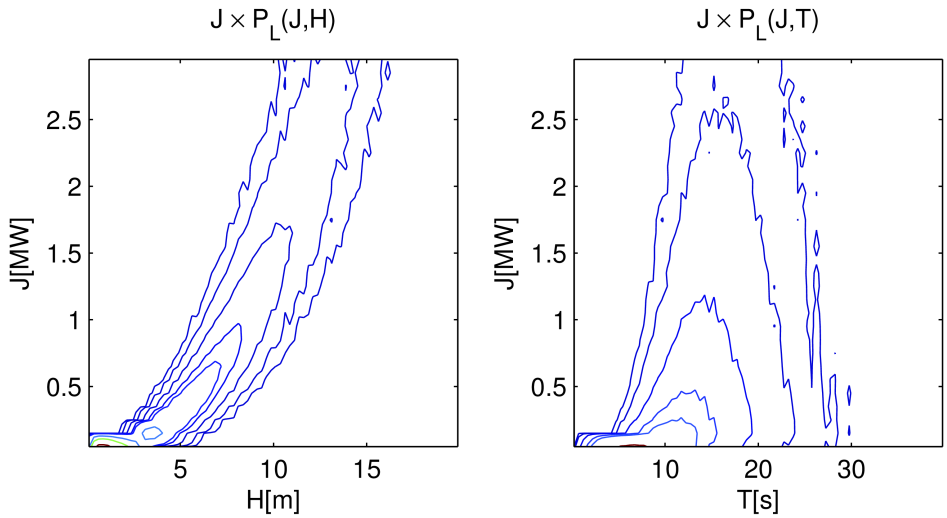

Figure 3.4: Plot showing $J \times p_L(J, H)$ and $J \times p_L(J, T)$ from the scatter diagram, where the contours are 0.00001, 0.0001, 0.001, 0.005, 0.01, 0.05, 0.1 and 0.2.

Figure 3.4 presents $J \times p_L(J, H)$ and $J \times p_L(J, T)$ from the scatter diagram. The difference between this and the results shown in figure 3.2 is not very large. However the important difference is that waves with higher energy will give more energy output per wave and therefore be more important than waves with less power. The contours are not so steep when the wave power is taken into account, as the largest values becomes smaller and the smallest values becomes larger. Even though the wave power is taken into account it is still the smallest waves that gives the largest contribution in the long-term perspective. When looking at the plot from the analytical calculations in figure 3.5 and comparing to figure 3.3 the same trends can be seen. A thing that becomes more clear in that plot is the variation of $J \times p_L(J, T)$ for low wave energy. As the wave period increases the contours will bend inwards because of the low wave energy, and not follow the symmetric shape seen for $p_L(J, T)$.

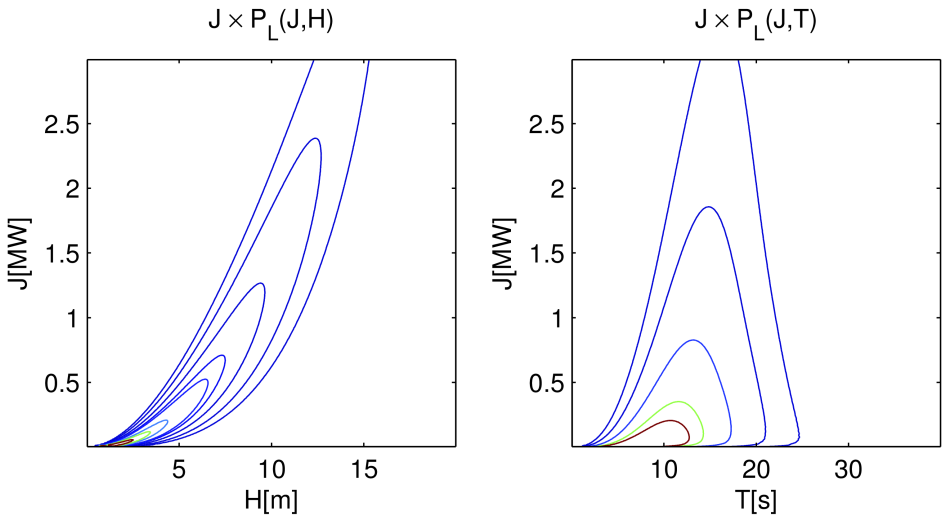

Figure 3.5: Plot showing $J \times PLJH$ and $J \times PLJT$ calculated from analytical expressions, where the contours are 0.00001, 0.0001, 0.001, 0.005, 0.01, 0.05, 0.1 and 0.2.

3.3.5 Long-term marginal pdf of wave power

It would be interesting to see how the wave energy is distributed when isolating the wave height and wave period. The long-term probability density function of only J can be found out of the long-term distribution $P_L(J, X)$. By integrating over the wave height or wave period this is found by

$$p_L(J) = \int_0^\infty p_L(J, X)\mathrm{d}X \tag{3.12}$$

where X is either the wave height H or the wave period T and $p_L(J, X)$ is the long-term distribution of J and X. As the long-term distribution $p_L(J, X)$ is found both from scatter diagram and analytical calculations, and is also calculated both with integrating over wave height and wave period, the long-term distribution of J can be found by four different methods. This can be used to compare and ensure the results already found.

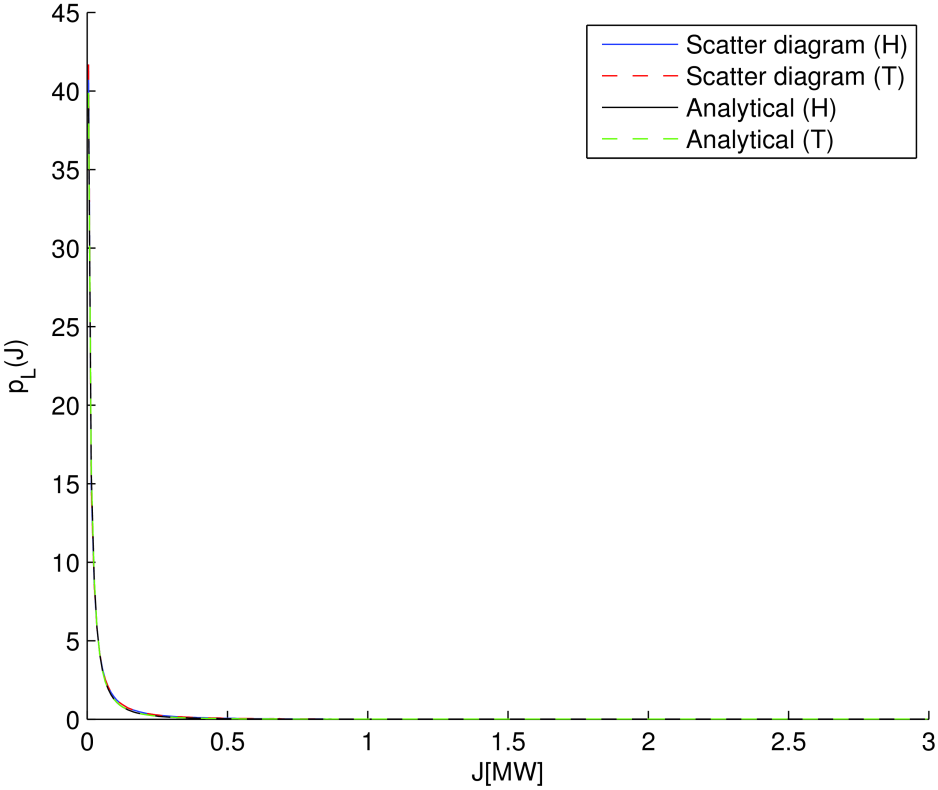

Figure 3.6: Long-term distribution of J, calculated in four different ways.

In figure 3.6 the long-term distribution of the wave power is plotted. It shows, as expected, a very steep curve, with large probabilities for low values of J. This is comparable with the exponential behaviour suggested with the assumption of narrow banded waves in chapter 3.1.

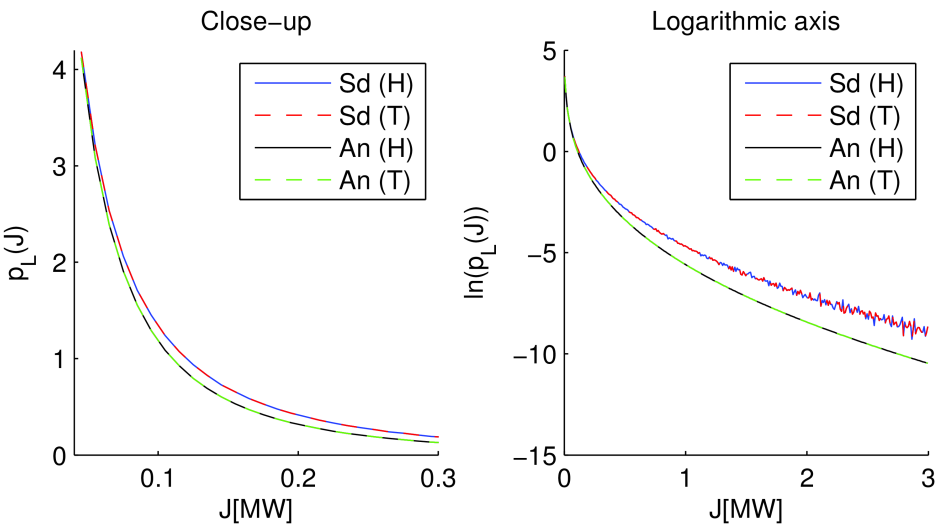

Figure 3.7: Long-term distribution of J, calculated in four different ways, presented with a close-up caption on the left and with a logarithmic vertical axis on the right

When comparing the different methods to calculate the distribution of J it is very difficult to see any differences. In order to maximize the differences $p_L(J)$ have been plotted both with an close up view and with an logarithmic axis, as presented in figure 3.7.

In the close-up figure it is seen that the analytical solution gives a little lower value than the scatter diagram calculations. But that is expected because there have been differences also in previous calculations. It is seen that the distribution found from the scatter diagram is the same if it is integrated from $p_L(J, H)$ as if it is integrated from $p_L(J, T)$. This suggests that the method used for finding the distribution is correct. The same is seen for the results that is found from the distribution made based on formulas.

The shape of the curve appear to resemble a exponential curve when looking at the close-up figure, but that would mean that the curve plotted with the natural logarithmic axis would be linear, and it is not. So it seems that the wave energy is not distributed exponentially.

In figure 3.8 the distribution of J found from the scatter diagram values is plotted with two analytical expressions. The first is a exponential distribution, with the shape $p_L(J) = ke^{\nu J}$ where ν and k is shape parameters, which is attempted to fit. However, as already seen, it does not have the same shape as the actual distribution. The exponential distribution gives higher probabilities for low values

of J, and lower probabilities for higher values of J. Another attempt of looking at the distribution is looking at the fact the graph looks very symmetric. By that a inversely proportional behaviour of the shape $p_L(J) = \frac{1}{kJ}$ where k is a shape parameter, is assumed. As can be seen this fits much better, especially for low values of J, but it gives a bit high values for increasing wave energy. To sum up none of these simple analytical expressions fits perfectly, so it cannot be said that the distribution of J varies either exponentially or inversely proportional, even though it have some similarities.

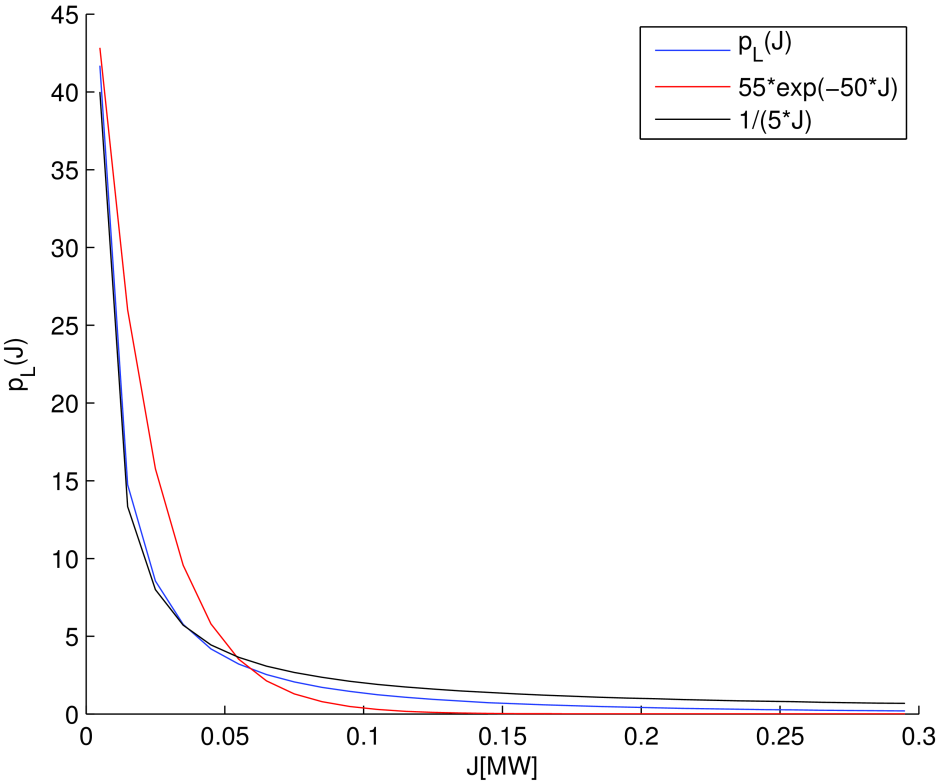

Figure 3.8: Plot of $p_L(J)$ compared to the analytical expressions $55e^{-50J}$ and $\frac{1}{5\times J}$.

3.3.6 Long-term marginal pdf of wave height and wave period

The same that is done to find $p_L(J)$ can be done to find the long-term distribution of H and T separated from J. Then the equation will be

$$p_L(X) = \int_0^\infty p_L(J, X)\mathrm{d}J \tag{3.13}$$

where X is either the wave height H or the wave period T. This is visualized in figure 3.9. When comparing the distribution of wave height from scatter diagram and analytical calculations it is seen that they follow each other good for large values of wave height. The main difference is however at the peak where the analytical calculations gives a much larger value, and for very small values where the analytical calculations goes to zero, and the scatter diagram calculations decreases from the peak more slowly. When comparing the distribution of wave period from the scatter diagram and analytical calculations it fits better. But also here it is seen that the formulas give a higher peak, but a little less values for the other areas.

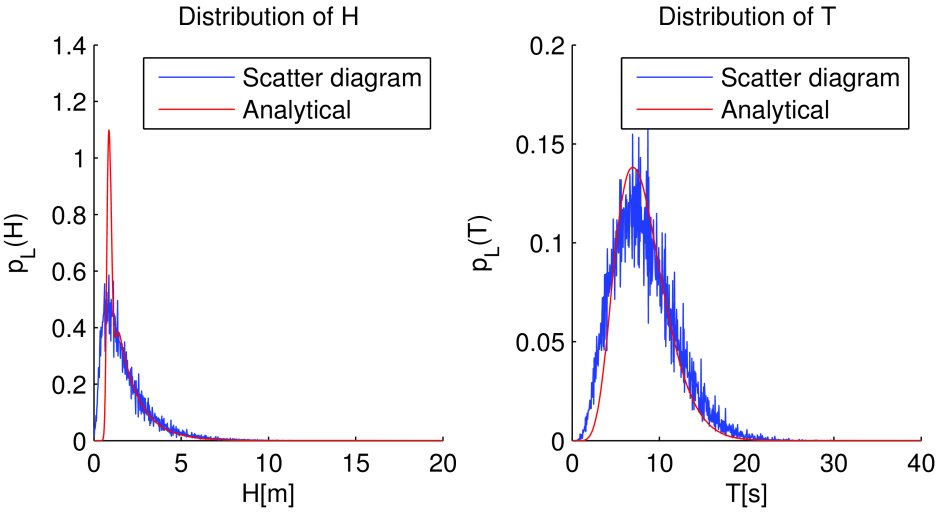

Figure 3.9: Long-term distribution of H (left), and long-term distribution of T (right), calculated from scatter diagram and from analytical expressions

3.3.7 Long-term CDF of wave power

When the long-term probability density function of J is found, it can be used to find the cumulative distribution function of J. This is found by

$$F_J(\hat{J}) = p_L(J \leq \hat{J}) = \int_0^{\hat{J}} p_L(J)\mathrm{d}J = \sum_0^{\hat{J}} p_L(J) \tag{3.14}$$

where $P_L(J \leq \hat{J})$ represents the probability that the random variable J takes on a value less than or equal to $\hat{J}$. The plot of these calculations is given in figure 3.10. Also here it is calculated in four different ways. As before there are no differences based on if the values are integrated for wave height or wave period. The difference between calculations from scatter diagram and formulas is still present and is as expected the same as the difference for the integrated total area described in table 3.1. In other words the scatter diagram values goes up to 0.99 and the formula values goes up to 0.95. It is seen that the graphs increase very rapidly in the start. This is, as mentioned before, because most of the waves have very low energy.

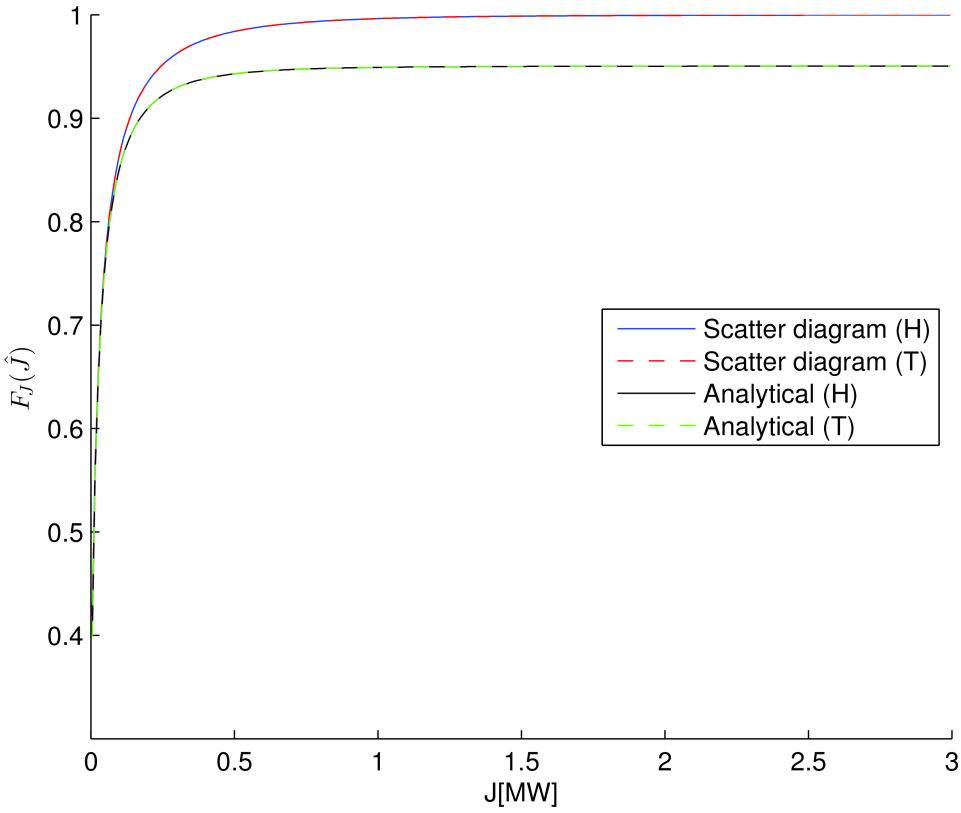

Figure 3.10: Long-term cumulative distribution of J calculated both from scatter diagram and analytical expressions.

Chapter 4

Control systems and power absorption

In the sea, it will over time be many different waves and sea states. The response of a WEC in the sea depends on the motion of these waves. It is therefore beneficial to have a WEC with response characteristics that takes advantage of the full potential in the waves, i.e. have its maximum output for the present waves. But because the characteristics of the waves change, this also means that the response characteristics of the WEC need to change. This leads to the idea of device tuning, i.e. the response properties of a WEC are changed to match the present waves by controlling different parameters in the WEC.

Device tuning can roughly be put into three categories [10]: Fixed tuning, slow tuning and fast tuning. Fixed tuning is that the device is designed with constant properties that give an overall good match for the range of waves in the area. Slow tuning is to change the WEC's parameters in minutes or hours to match the different sea states. Fast tuning, or wave-by-wave tuning, is to change the WEC's characteristics for each wave or small sequences of waves.

Tuning the device to each individual wave could give an significant increase in extracted power. There is many ways of doing this, but in general it demands complex software algorithms, sensors and controllers, and could therefore be difficult. It has to be considered how to get maximum power but still have a usable, not to complex device. Tuning for each wave will theoretically give more power, but also introduce technical difficulties to make it possible because of the rapid changes and calculations that are needed to be done. The best solution might be to tune the device to a range of waves, to get a satisfying power extraction level, but without having a to complex system.

The main reason for device tuning is as mentioned to get as much power out of the waves as possible. Hals [3] describes this a little more thoroughly by introducing some criteria. He divides into two main control aims. The first is to maximise the average power output under the limitations set by the equipment. The second is to maximize the average power output set by the capacity of the energy converter. Hals [3] also introduces some other criteria for device control. The control system should protect the device and its machinery under severe storm conditions and it should help to give safe operation under failure situations, and safe shut-down if necessary. In order to utilize the capacity of a device it also needs to be designed in a appropriate size. Increased control of the device will result in an increase in average oscillation amplitude, and preferably the device should be designed to work at a full stroke for a substantial part of the operational time, so that the volume of the structure is exploited.

4.1 How to control the motion of a device

The are many ways of doing this control of motion. In general a typical goal would be to change the natural frequency of the WEC to match the waves, by changing such things as the size, shape, weight, stiffness or damping depending on what is possible for the specific device. Hals [3] defines the key control variable for controlling the motion as the machinery force. There are many different ways of define the behaviour of this force. One way is to assume that it has linear behaviour, but if the force should include some effects to describe different abilities, non-linear behaviour has to be introduced. Hals [3] describes three different categories for the machinery force.

The first is resistive loading, which means that the machinery force only are able to extract power from the system, which means it cannot do work to the system as a motor. By having a constant resistance of the system the machinery force becomes linearly dependent on the velocity. By introducing a time-dependent resistance effects such as latching and clutching (which will be explained later) can be introduced.

The second category is Reactive loading, which means that the machinery forces can be proportional to for example position and acceleration, which means that the machinery force can work partly as a motor.

The third category is Non-linear loading, which means that no initial restrictions are put on how to represent the machinery force. This would typically include machinery forces with non-linear feed-back terms, switching controllers or online numerical optimisation. This will give the possibility of constraint handling.

Another control mechanism that is necessary is restriction for maximum stroke.

Because most WEC's needs a restriction on the maximum stroke of moving parts they have physical end stop mechanisms. Similarly virtual end stops can be incorporated in the controller. This is known as constraint handling. The main goal of this is to avoid that the moving parts reach the physical end stops, or to reduce the impact when the limits are reached.

4.2 Different control systems

Hals et al. [4] describes many different concepts for control systems. The question is, as described, how to control the machinery force. The different concepts and the main principles of how they work are described in the following. All of the control concepts use different strategies of control, thus they might not work on every type of WEC because the application of the control mechanism can be difficult or it has to be done in a slightly different way. The basic concept is however the same, and that is way it is described here.

4.2.1 Resistive loading (RL)

A simple way of modelling the machinery force is to assume that it depends linearly on the velocity, thus having ha constant resistance. As described earlier this is called resistive loading. This is not very much used in real life, but often useful as a starting point in modelling and simulation studies as well as laboratory experiments and prototyping. This would also be a good reference when comparing to more advanced methods. In this case the machinery never has to work as a motor.

4.2.2 Approximate complex-conjugate control (ACC)

Maximum useful absorbed energy for a body oscillating in one mode is achieved provided that the intrinsic reactants are cancelled and that the load resistance equals the intrinsic resistance. The word intrinsic is used to signify the systems own impedance terms, including friction and viscous losses, but excluding machinery forces. One way of achieving this is complex conjugate control. The name comes from the way of calculating this, but the details are beyond the scope of this thesis. However this condition may equivalently be expressed by two requirements that are easier to understand figuratively:

- Optimum phase: The body must oscillate with its velocity in phase with the excitation force.

- Optimum amplitude: The oscillation amplitude must be adjusted such that the radiated power equals half the excitation power.

This is called phase and amplitude control, and is an easier way of explaining the same goals as complex-conjugate control.

Complex conjugate control corresponds to providing a direct feedback from the velocity of the buoy. But there is a problem with this way of finding the optimum, because the optimal control force becomes dependent on future values for the excited force. This is impossible to implement in practice, because the velocity is dependent on the future choice for the machinery force. This can however be solved by predicting the future based on local measurements or computing it from remote measurements. Another solution would be to assume some of the values to be constant and in that way find a simple approximation. This is called approximate complex-conjugate control. In this method the machinery has to handle a reactive power flow so it falls into the category of reactive control.

4.2.3 Tracking of approximate optimal velocity (AVT)

Phase and amplitude control can be seen as a velocity tracking problem. Then the problem will be how to approximate the optimal velocity function. One way would be to assume a constant resistance, and in that way achieve an approximation. This is the basic thoughts of the control mechanism called tracking of approximate optimal velocity.

4.2.4 Model-predictive control (MPC)

A way of control the machinery force based on prediction of the future is described by model-predictive control. The idea is to optimise a short future expected response of the system. This is done by using a discrete-time model of the WEC together with a prediction of the input force. As the time is running the time window for the predictions is moved along, and the optimisation may be solved at predefined intervals. This will give the best control force at each instant given the instantaneous states and conditions.

4.2.5 Phase control by latching (PML and TUL)

Latching is a control strategy to achieve optimum phase without having to supply reactive power. The idea is that the motion is stopped during parts of the cycle,

with a latching mechanism, and power is taken out during motion. The typical way of doing this is to latch the motion when the velocity becomes zero, in other words, when the device is at the extreme position, and unlatch at the right moment for the velocity to fall into phase with the excitation force. The power is then harvested during the transition between outer steady positions.

However the challenge is to determine the instant of unlatching, as it depends on future values for velocity and excitation forces. Different attempts have been proposed to get a good enough accuracy. One of them is the *peak-matching latching control* (PML) where the aim is to match the peaks of the force and the velocity signals. This is achieved by releasing the WEC approximately $T_0/4$ before the next predicted peak for the wave force. Another attempt, called *threshold unlatching control* (TUL), releases the WEC once the force passes a chosen threshold value. This does not rely on predicted values for the excitation, but of an estimation of the instantaneous excitation force. A challenge to get this to work in real life is to design a durable method or mechanism that can successfully do the latching and unlatching.

4.2.6 Phase control by clutching (PMC and TUC)

A very similar control mechanism to latching is clutching. The idea is that the machinery is engaged only during parts of the cycle, and the device is oscillating freely otherwise. The typical way of doing that is to engage the machinery at zero velocity, and disengage it in time for the velocity to have the same phase as the excitation force. So the difference between this and latching is that instead of the motion being locked, the WEC is moving freely during parts of the oscillation cycle. The power is harvested during a slow sliding motion from the outer positions.

Similarly as for latching, it is also for clutching difficult to determine the instant of coupling the machinery. The two different attempts to solve this for latching can also be used for clutching, namely called *peak-matching clutching control* (PMC) and *threshold unclutching control* (TUC). Also for clutching is the design of a durable method or mechanism to do the coupling and uncoupling considered a challenge.

4.3 Comparing the different control systems

For the comparison between the different control systems it have been done with a heaving sphere with a power take-off system, where the energy is extracted, connected between the sphere and a fixed reference, as shown in figure 4.1. The comparison is done both in regular and irregular waves.

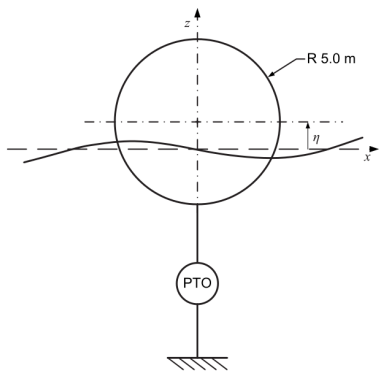

Figure 4.1: Illustration of the heaving sphere energy absorber used by to compare control concepts by Hals et al. [4]

In regular waves the differences between the methods are very small. All methods will perform relatively well because the future is known. However it is worth noticing that the RL case performs poorly at regular waves. But the results in regular waves are not that important, as irregular waves are the conditions that these control systems is supposed to handle.

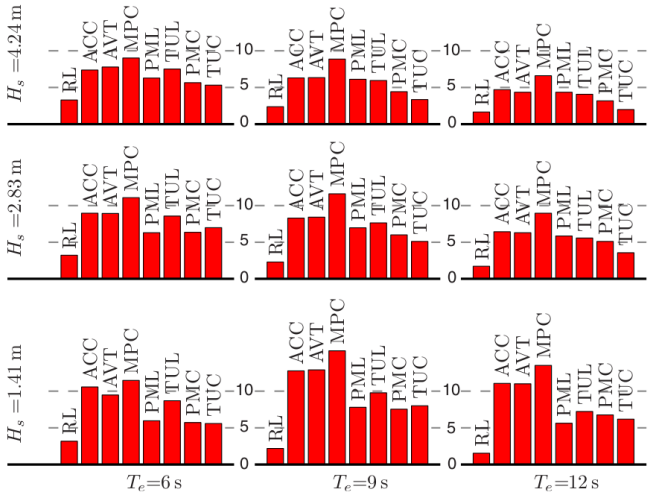

Figure 4.2: Absorption width $d_a = \overline{P_u}/J[m]$ (based on absorbed useful energy) in irregular waves for different control strategies. Horizontal dashed lines are drawn at $d_a = 5m$ and $d_a = 10m$. Copied from Hals et al. [4].

The comparison results for irregular waves from Hals et al. [4] is given in figure 4.2, where the absorption width, based on the absorbed useful energy, is presented. All controllers give significantly more power than the RL case. As expected the MPC controllers gives the superior performance in terms of converted power. ACC is the second best, slightly better than AVT. Latching and clutching generally have similar results. For smaller waves the latching and clutching strategies are significantly weaker than the reactive control algorithms. But when wave height increase, the difference reduces, or even vanishes. It is seen that for the threshold strategies of latching and clutching the TUL gives a little higher values than the TUC. Clutching gives larger power dissipation in the end stops than the other controls, if that maybe could be converted to useful energy the differences between latching and clutching would be reduced, but not cancelled. Hals et al. [4] also observes that the absorption width is decreasing width increasing wave amplitudes/heights. The reason for this is that the amplitude restriction for the device as the wave height increases will have increased influence.

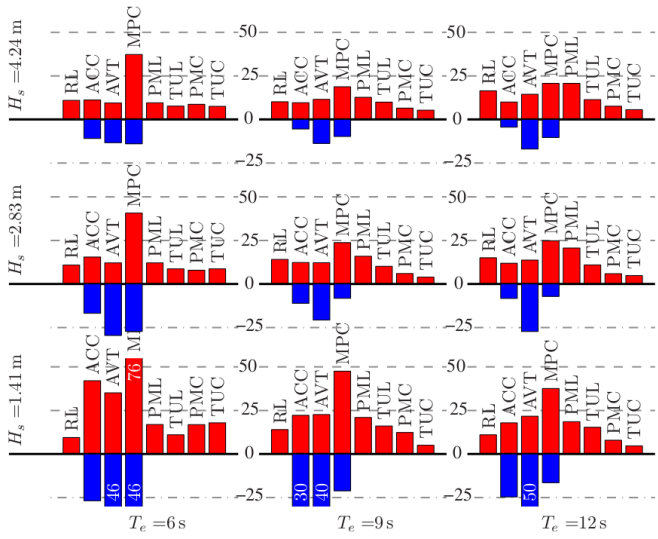

Figure 4.3: Peak-to-average ratio for the power flowing through the machinery of incident irregular waves, corresponding to figure 4.2. Horizontal dashed lines are drawn at the values -25, 25 and 50. Some bars go outside the scale, their sizes are given with the white numbers. Copied from Hals et al. [4]

Hals et al. [4] also compares the peak-to-average ratios for the absorbed power for the different control systems. The peak-to-average ratios are given as the ratio between maximum or minimum value divided by the average value for the absorbed power. In other words it is used to describe the variations of absorbed power within

a sea state. The negative ratios describe a control system when the machinery does work as a motor. High ratios will be demanding for the machinery in the control system, because it needs to handle large variation in power, and it will need a good design to meet this challenge.

It is interesting to see the large peaks for the MPC. For the ACC it is interesting to see that the negative ratios is of same magnitude as the MPC, but the positive ratios is much smaller, and the reduction in converted power (from figure 4.2) is very modest. This means that the ACC could be very attractive when comparing to MPC when the design of the machinery is also considered. But the MPC have an advantage in the possibility of including constraint handling, thus the large peak-to-average ratios can be reduced. However this will off course lead to a reduction in absorbed power for the MPC.

The clutching strategies have very low ratios. As clutching does not have reactive power flow (negative ratios) clutching seems like a very good alternative if a good machinery design is used. Latching generally gives ratios comparable to the ACC and AVT controllers. When looking at latching and clutching, it is seen that the threshold strategies give lower ratios than the peak matching algorithms.

If the results are summed up some interesting conclusions appear. It is seen that to supply the computed machinery force a large reactive power through the machinery is needed. this can be challenging because this means that the machinery have to be designed for a much larger instantaneous power than the average power that the WEC is able to deliver. This means that if the intention is to apply reactive control an energy storage would be needed.

Although latching and clutching is inferior to the best control systems when it comes to absorbed power, they have some interesting advantages. They do not require reactive power flow through the machinery, and due to the low peak-to-average power ratio the total results is able to compete with the best.

To make a definitive conclusion of which of the control systems that is the best is difficult because they perform different for different comparisons, and each system has its advantages and disadvantages. What is the best system will therefore probably be different depending on what WEC it is used with and the waves that will occur. However the knowledge presented here would be helpful when comparing different methods.

Chapter 5

Power Absorption for energy converters

When a WEC is placed in water its task is to absorb energy from the waves. That is why it is put there, and that is what it is designed to do. In other words, how good it absorbs energy, and for what range of waves it is effective should be thoroughly studied. This would reveal advantages and disadvantages for different WEC's in different types of waves, and it would give important knowledge when developing and improving a WEC.

There exists WEC's of many different shapes and sizes. Different concepts is described by Hagerman [2] and McCormick [6]. The WEC's take advantage of different properties of the waves and they are optimized for different locations and wave patterns. All of this makes it difficult to compare different concepts with each other in a objective way. And it does not help that most of the needed information, like energy absorption, dimensions and costs, is unavailable from the manufacturers. An attempt has been done in Babarit et. al [1]. By taking the information that are available and assume the dimensions of the WEC based on pictures, Babarit et al [1] are able to estimate some quantities. They are used to define four different criteria for comparing different WEC's:

- Energy absorption
- Energy absorption / tons of displacement
- Energy absorption / square meter of wetted surface
- Energy absorption / unit of significant power take off force

The energy absorption has been analysed numerically, using dimensions that have been assumed. These criteria could give a overview of the different WEC's advantages and disadvantages, and an indication of which is the better one.

However Babarit et al. [1] acknowledges that the ultimate criterion is the cost of electricity per kilowatt hour. This depends on two main criteria which is the output power and the total cost of the system including everything. The cost of the WEC is difficult to find because manufacturers keep it secret, and it is also generally not known because no one have ever produced WEC's in a large scale and experienced what it would have cost. Because no data of cost exists it is also very difficult to assume something and make an estimate.

The output power, on the other hand, can be estimated analytically by known theory of hydrodynamic forces. This is what Babarit et al. [1] has done with four different WEC's. This has been done by using linear potential theory with mono-directional waves, a power take off system which is assumed to have a linear behaviour and the WEC's are optimized for each sea state (slow tuning).

5.1 Different concepts

The four different WEC's is all different in how they exploit the energy in the waves. Comparing them could give an indication of what kind of concept that is best, or at least some differences in what conditions they perform best.

5.1.1 Heaving buoy

The first WEC is a heaving buoy, presented in figure 5.1. The buoy is following the surface, and is connected to the sea bed in the other end via a pump. The pump is capturing the relative movement between the buoy and the sea bed, and the energy is absorbed. The buoy should be small and have a natural frequency much lower than the waves, so that it follows the waves as much as possible.

5.1.2 Heaving two bodies system

The heaving two bodies system, presented in figure 5.1, consists of two bodies moving relative to each other because they follow the waves differently. The two bodies consist of a bigger and deeper body referred to as the float, and a shallower circular body referred to as the torus. Compared to the heaving buoy, this device is much larger.

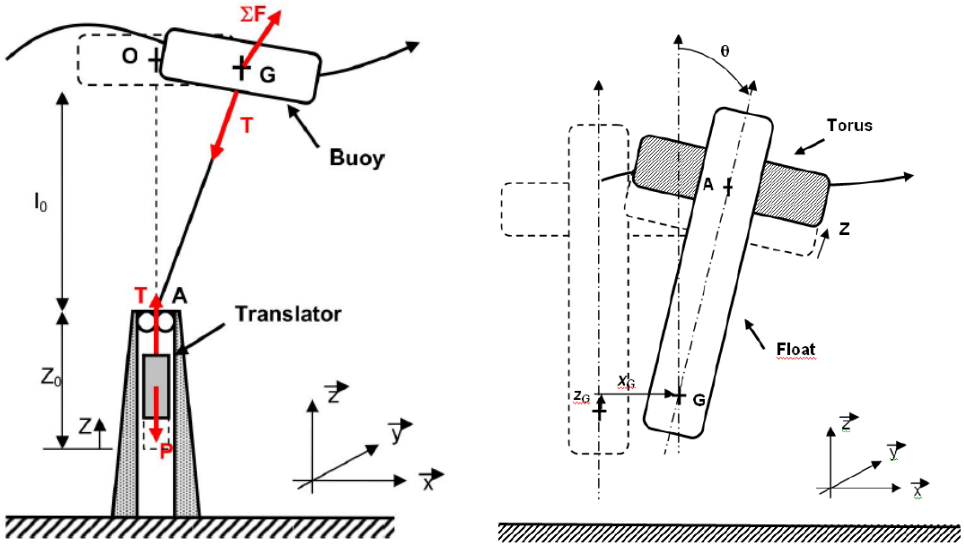

Figure 5.1: left: Sketch of the heaving buoy [1]. right: Sketch of the heaving two bodies system [1].

5.1.3 Pitching device

The forces in a wave have sinusoidal changes, and therefore half a wavelength apart there is velocities in different directions. These counteracting forces in different phases of the wave are possible to use for energy conversion. An example of that is the pitching device Langlee, as shown in figure 5.2. The device is a floating structure with two sets of flaps at a distance of half a wave length (optimally), thereby counteracting. As they move in opposite directions they move a hydraulic system connected to electric generators.

5.1.4 Floating OWC

There exist numerous attempts of wave energy converters that exploit a moving water column as a piston in a cavity. The floating OWC, presented in figure 5.2, is known as the backward bent duct buoy. The idea is that a cylinder with openings in both ends is placed in the water. Incoming waves will lead to different pressures, and an oscillating water column inside the cylinder. The opening in the top is closed by a valve connected to a turbine. When the water column moves up and down as a piston in a motor, it would pressure the air pocket through the valve to

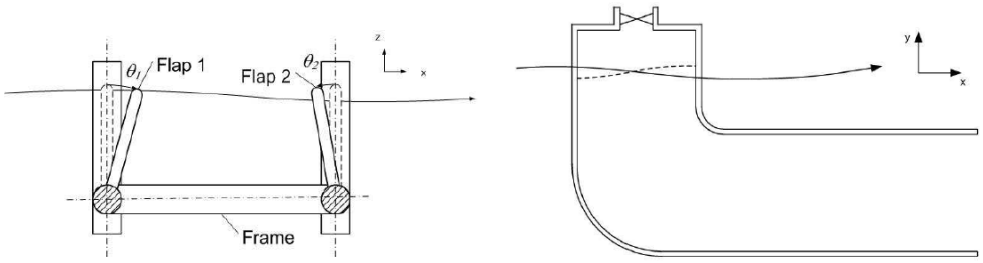

Figure 5.2: left: Sketch of the pitching device [1]. right: Sketch of the pitching OWC [1].

run the turbine.

5.2 Computation of efficiency

The energy absorption for different WEC's could be presented as how much energy they can absorb for different sea states. For increasing H_s and T_p the absorbed energy will increase, but the percentage which is absorbed of the total available energy will vary differently. This would be individual for each WEC. Then it would be interesting to see how the differences between the WEC's are, and which is better. A good ability for a WEC would be the ability to absorb a large portion of the wave power present for a given sea state. In other words it is beneficial for the WEC to have high efficiency. This could be found by comparing the absorbed power for the WEC with the theoretically wave power for a sea state. The theoretically power in a sea state is given by [7] as

$$J = \frac{\gamma g^2}{64\pi} H_s^2 T_j \tag{5.1}$$

where $\gamma = 1025kg/m^3$, $g = 9.81m/s^2$, H_s is the significant wave height and the wave energy period is given as $T_j = 0.91T_p$ where T_p is the spectral peak period. From the formula it is seen the energy will increase with the square of the wave height and linearly with the wave period. So the energy will increase rapidly and have much more energy in the sea states with larger waves.

The energy absorption, given as a function of H_s and T_p, for the different WEC's is found by Babarit et al. [1], and are approximately redrawn to be able to do calculation with them. This means that the numbers would not be exact, but they will describe the general trend. However for smaller waves, where the energy could

be close to zero it is difficult to assume the value, because a large part is plotted with the same color. This could for some values give very wrong results if the value is redrawn with a too large value, and the efficiency could be calculated to be very high, when there in reality is no energy absorption for that sea state. This could even lead to efficiencies larger than one.

Efficiencies large than one is however not impossible. This is because the power absorption is dependent on the width of the area of waves that is absorbed from. This width could be smaller than the width of the WEC, but it can also be larger. This is due to focusing techniques as described by McCormick [6]. Wave focusing techniques is in general the use of techniques to focus the wave energy into a smaller area in order to increase the power density in the waves. This could be divided into three main concepts [6]; the antenna, island focusing and lens focusing. The concept of the antenna, as shown in figure 5.3 for a heaving buoy, is similar to what happens to radio signals. The theory of 2D waves says that a heaving buoy only can extract half of the wave energy. But when looking at a 3-dimensional situation the width of influence also have to be taken into account. If the buoy is in resonance with the waves, a wave crest of width $\lambda/2\pi$ will focus its power into the buoy. This width could be significantly larger than the diameter of the buoy, and the possible power output could therefore theoretically be larger than 100% of the wave power available in the area covered. The other focusing concepts have practically the same goals as antenna focusing but use other methods to achieve focusing of the wave power.

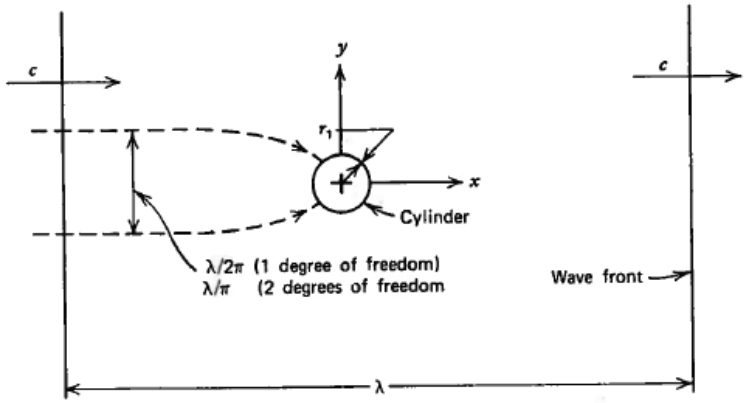

Figure 5.3: Sketch of the concept of antenna focusing from [6]

In the following calculations the width of influence is assumed constant as the width of the WEC. This would not be exactly true because the width of influence will vary with the sea states, and different types of WEC's might have individual differences which make the assumption that the width of the WEC is the same as

the width of influence not correct. However it is still a reasonable assumption to make.

5.3 Results

For the heaving buoy the width of influence is assumed as the width of the buoy which is $1.5m$. The power matrix and efficiency is shown in figure 5.4. It can be seen that the power absorption increases very rapidly for increasing wave height. The heaving buoy absorbs most power for wave periods of seven to eight seconds. However as the wave absorption increases for increasing wave height and in some extent for increasing wave period it is for low values of these that the heaving buoy is most effective. This is not surprising because it will be very difficult to absorb a large portion of the power when it is as large as it is for increasing wave height and wave power. This is a general trend seen on all the WEC's.

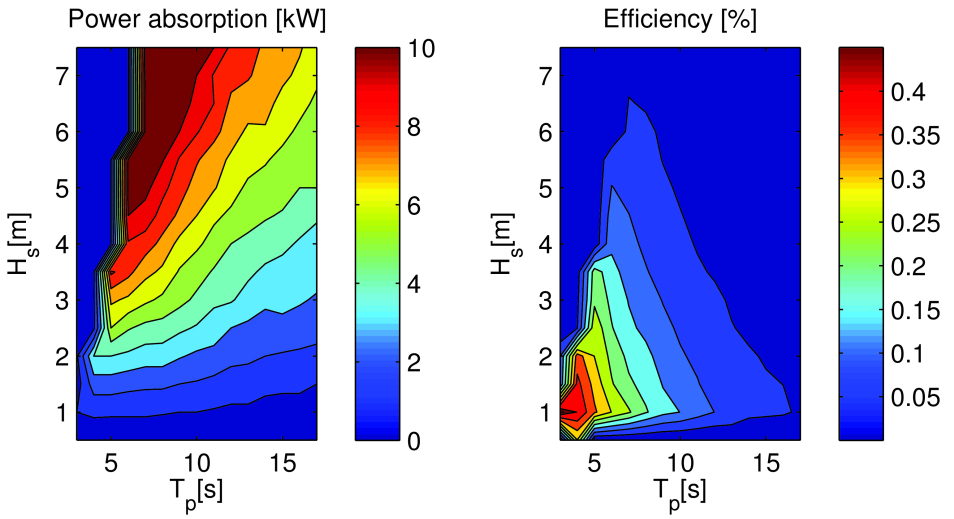

Figure 5.4: Power absorption of the heaving buoy and efficiency of the total available power.

For the heaving two bodies system the width of influence is assumed as the width of the torus which is $20m$. The power matrix and efficiency is shown in figure 5.5. It can be seen that the power absorption is increasing to its max potential around $T = 10s$ and for increasing wave height. When focusing on the efficiency it is seen that it is largest for the same wave periods but at lower wave heights of one to two meters.

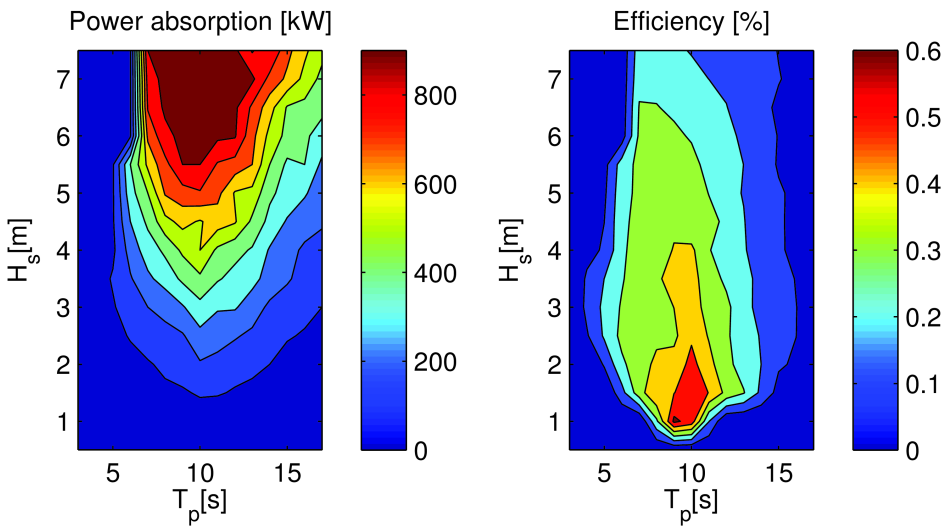

Figure 5.5: Power absorption of the heaving two bodies system and efficiency of the total available power.

For the pitching device the width of influence is assumed as the width of the whole frame which is $25m$. The power matrix and efficiency is shown in figure 5.6. It can be seen that the power absorption varies similarly to the heaving buoy except that is it more dependent on the wave period. The efficiency is largest for wave period of around eight seconds, and low wave heights.

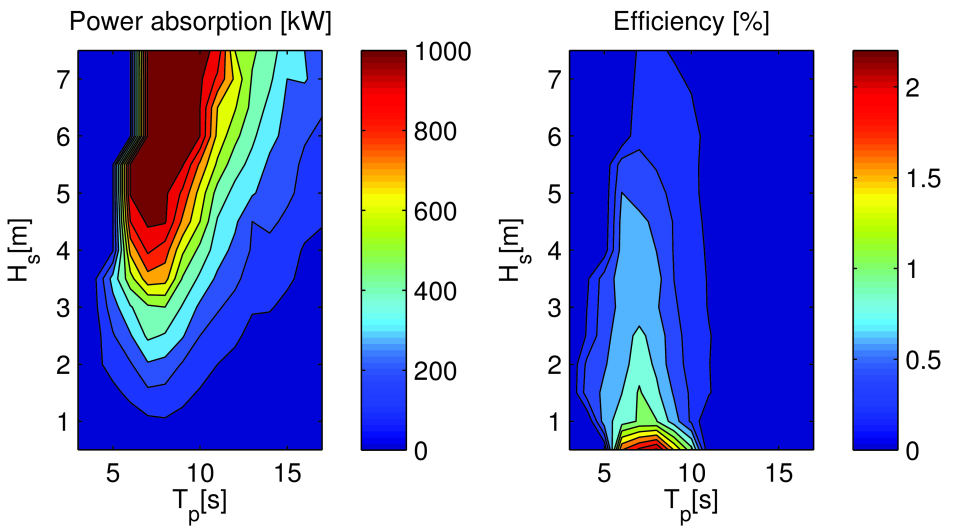

Figure 5.6: Power absorption of the pitching device and efficiency of the total available power.

For the floating OWC the width of influence is assumed as the width of the device which is $24m$. The power matrix and efficiency is shown in figure 5.7. The power absorption increases for increasing wave height, and it has quite small variations of power absorption for changing wave periods. Compared to the other WEC's the area giving high energy output is larger. The efficiency is largest for wave period of seven seconds, and is almost independent on the wave height until they get large.

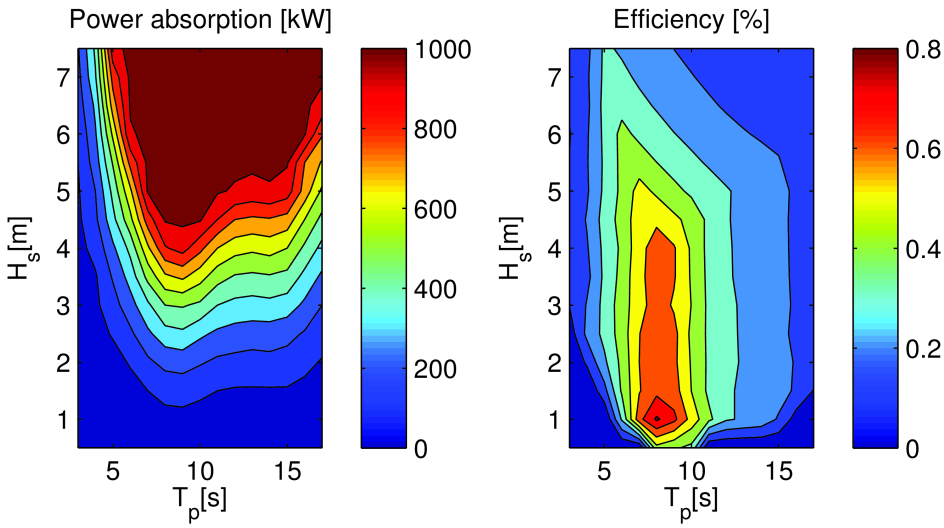

Figure 5.7: Power absorption of the floating OWC and efficiency of the total available power.

When looking at all the WEC's it is seen that most of them are most efficient for one specific wave period, and that the efficiency is decreasing for increasing wave height.

When comparing the maximum percentage of absorption it is some differences between the WEC's. As the maximum of the heaving buoy is only at 45 % the pitching device gives up to 120 %. However these differences should not be overrated in importance as they come out of some coincidences. It is dependent on the width of influence which is just assumed, and also on the guesses that are made when the values are read from the figures in Babarit et al. [1].

In order to decide which one is the better one it should be compared with some real occurrence of waves, like long-term statistics. Because there is no need to be effective in a wave that never comes if the overall efficiency is poor. Long-term statistics will introduce knowledge of occurrence of sea states, thus telling at what sea states it is preferable to have large efficiency.

Chapter 6

Computation of long-term efficiency

In chapter 5 the efficiency of different WEC's for sea states is presented. By inserting this efficiency into the long-term equation, presented in section 3.2, long-term efficiency can be found. This is done by adding a efficiency term in equation 3.8 so that it will yield

$$p_{L,\eta}(J,X) = \sum_{i=1}^{\infty}\sum_{j=1}^{\infty} p(J,X \mid H_s,T_p)p(H_s,T_p) \times \eta_{H_s,T_p} w(H_s,T_z)\Delta H_s \Delta T_p \quad (6.1)$$

where η_{H_s,T_p} is the efficiency of a WEC for a given H_s and T_p, as presented in chapter 5. All the other terms are defined as before.

The efficiency is implemented so that the values are assumed to be zero where no data is available. It is reasonable to assume that the WEC's could be turned off when such extreme sea states occur, and they would probably also have a kind of end-stop device stopping these extreme states. However the calculations for individual waves still spans over larger wave heights and wave periods. This is mainly done because the program calculating it is made that way, but also because turning a device of under extreme conditions does not necessarily include shutting down for each extreme wave.

6.1 Long-term efficeincy of wave power, wave height and wave period

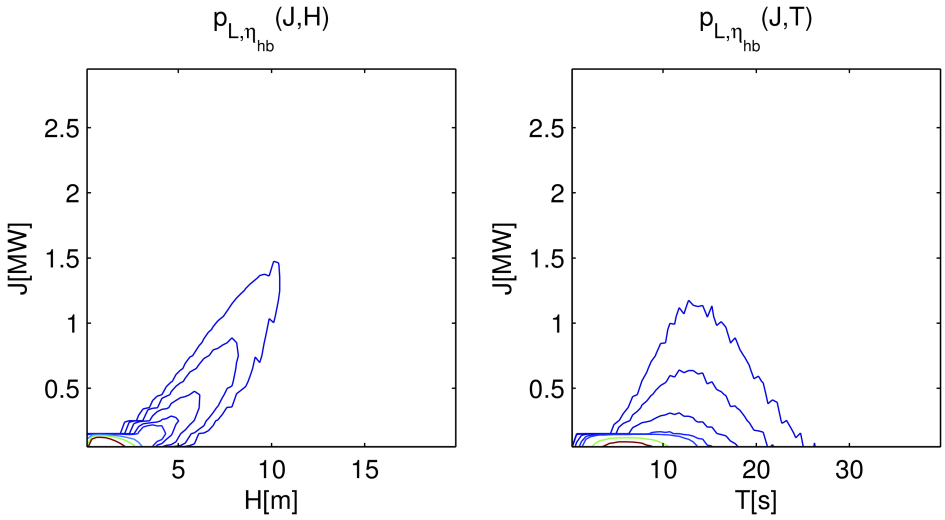

Figure 6.1: Long-term pdf of power absorption for the heaving buoy, where the contours are 0.00001, 0.0001, 0.001, 0.005, 0.01, 0.05, 0.1 and 0.2.

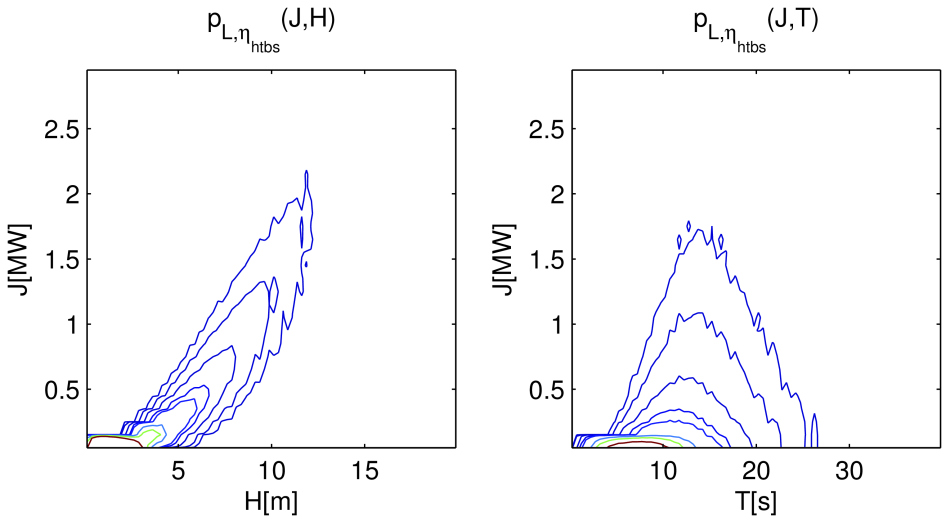

Figure 6.2: Long-term pdf of power absorption for the heaving two body system where the contours are 0.00001, 0.0001, 0.001, 0.005, 0.01, 0.05, 0.1 and 0.2.

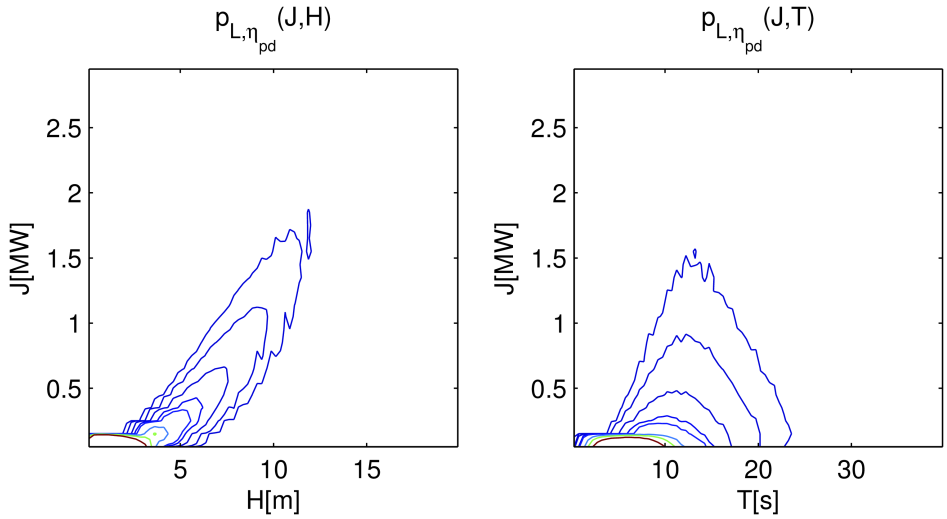

Figure 6.3: Long-term pdf of power absorption for the pitching device, where the contours are 0.00001, 0.0001, 0.001, 0.005, 0.01, 0.05, 0.1 and 0.2.

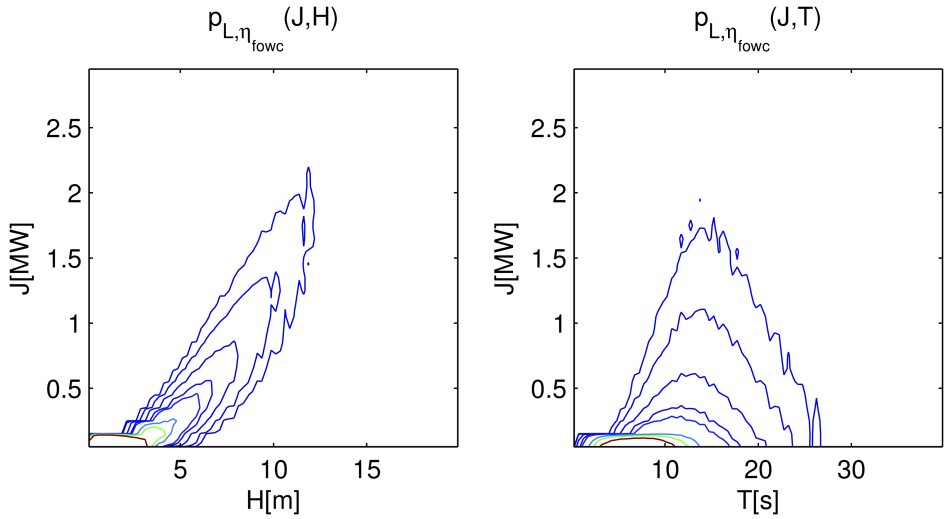

Figure 6.4: Long-term pdf of power absorption for the floating OWC, where the contours are 0.00001, 0.0001, 0.001, 0.005, 0.01, 0.05, 0.1 and 0.2.

In figure 6.1, 6.2, 6.3 and 6.4 the long-term pdf of power absorption are given for the WEC's presented in chapter 5. These are plotted with the same contours as in figure 3.2 which they could be compared to. However it is quite difficult to see

the differences in the plots. By looking at the outer contours it can be assumed that the heaving buoy gives the lowest power absorption, followed by the pitching device, and highest values are obtained for the heaving two bodies system and the floating OWC. But this way of putting it does not take into account which one is best for small waves, where most of the waves occur. So other ways of comparing them should be assessed.

Efficiency	$p_{L,\eta}(J,H)$	$p_{L,\eta}(J,T)$
Heaving buoy	0.1156	0.1156
Heaving two bodies system	0.3012	0.3012
Pitching device	0.4710	0.4710
Floating OWC	0.4376	0.4376

Table 6.1: Total efficiency for a long-term comparison

In table 6.1 the integrated total area of the power absorption is summed up in order to compare the different WEC's. When comparing the integrated total area of $p_{L,\eta}(J,H)$ and $p_{L,\eta}(J,T)$ it is seen that it gives the same results. This is good as it confirms the mathematical procedure. When comparing the different WEC's to each other it is seen that the pitching device and the floating OWC is the best by exploiting 47% and 44% of the potential, the heaving two bodies system exploits 30% and the heaving buoy is poorest by only 12%.

6.2 Long-term marginal pdf of power absorption

It would be interesting to compare them in other ways than only the total integrated area, and see how they vary for different wave power. Therefore the long-term marginal pdf of power absorption $p_{L,\eta}(J)$ is found. This is presented in figure 6.5. It is seen that the WEC's have very different results for low wave energy. The pitching device gives best extraction, followed by the floating OWC, the heaving two bodies system, and last the heaving buoy. However for larger wave energy it is the floating OWC that is best, and the pitching device goes down to the level the heaving two bodies system. The heaving buoy seems to be the poorest at every level of the extraction.

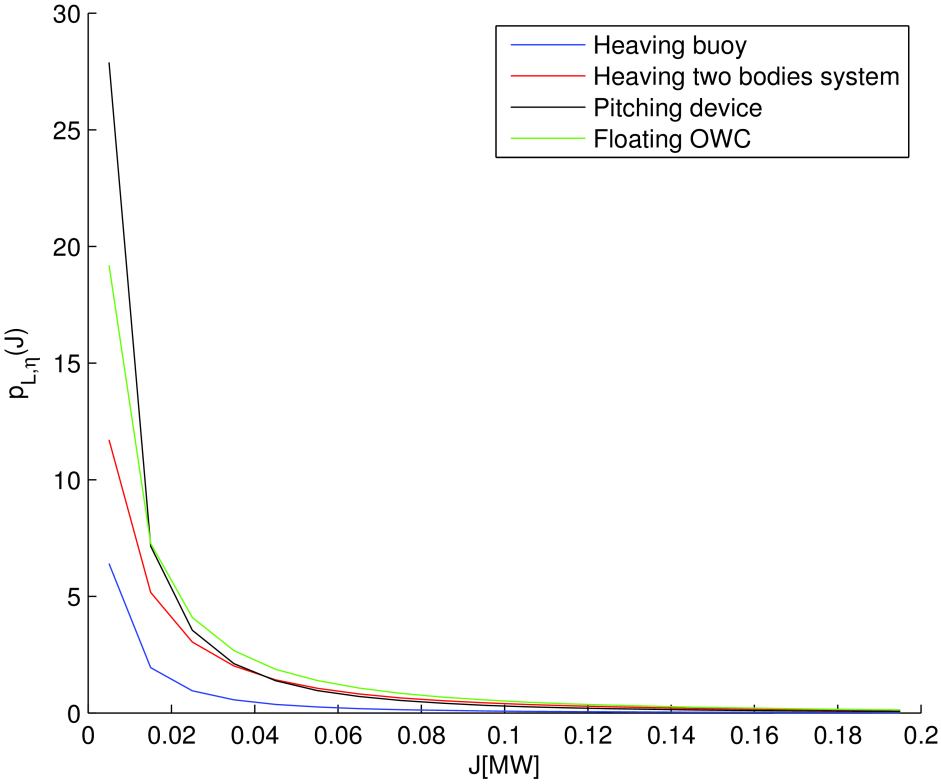

Figure 6.5: Long-term distribution of extracted wave power, $p_{L,\eta}(J)$.

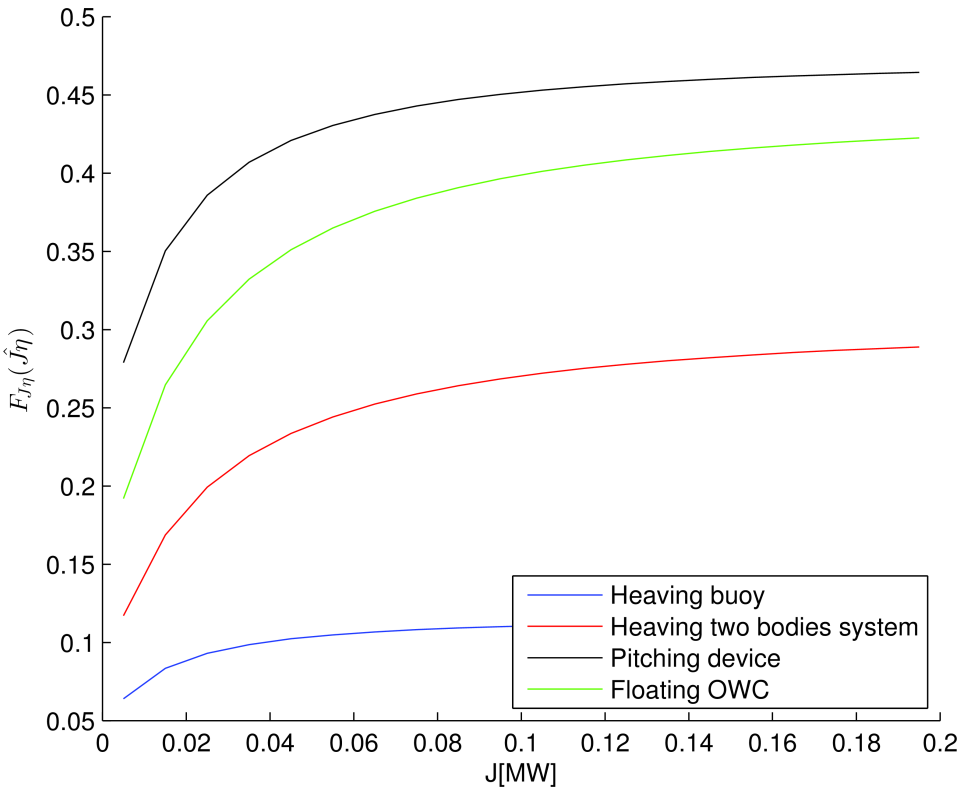

Figure 6.6: Long-term cumulative distribution of wave energy absorption.

6.3 Long-term cdf of wave energy absorption

Another way of compare them is to look at the cumulative distribution function, presented in figure 6.6. This shows the same overall results as before, with the pitching device as the best, and the heaving buoy as the poorest. However this shows that the pitching device is not as good as the floating OWC and the heaving two bodies system for larger wave energy because it increases less.

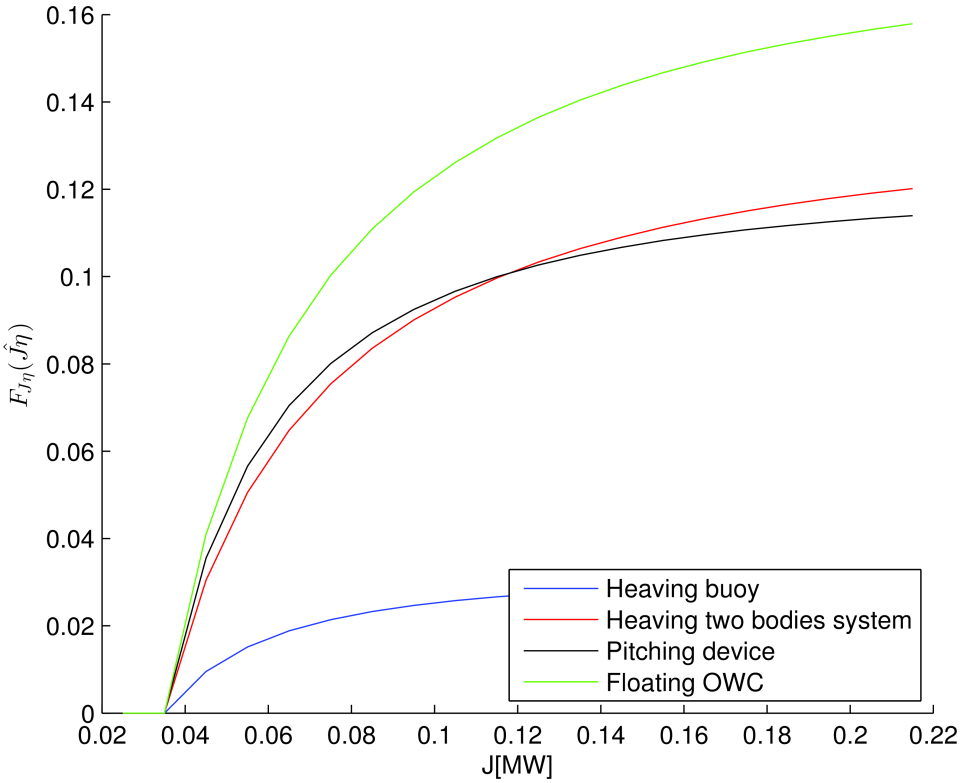

Figure 6.7: Long-term cumulative distribution of wave energy absorption where it is assumed no extraction for the lower wave energies.

As previously explained, in section 5.2, the power extraction for low values is not explained very clear in the original source [1]. Therefore it is possible that the low values are wrong. Therefore there have been made a plot where it is assumed that the power extraction for the lowest values of J is zero. This is where most of the waves occur. This is given in figure 6.7. From the figure it is seen that the heaving buoy is clearly not as good as the others. For the others they are very similar in the beginning, but the floating OWC stands out as the best.

Chapter 7

Conclusion

7.1 Results

When comparing the calculations done by use of scatter diagram and analytical expressions some differences are observed. In order to get correct results for the analytical expressions the resolution have to be high, so that peaks and values close to zero is included. But for the scatter diagram calculations the resolution is limited by the number of waves present in the wave scatter diagrams. If the scatter diagram results have too high resolution the results will become very fragmented and impossible to understand.

To include all the waves in the scatter diagram calculations the integration have to include a large enough span to involve the largest wave in the scatter diagram. If it does that the probability will sum up to 1. For the analytical expressions the integration in theory have to go to infinity to sum up to the probability of 1. But for numerical calculations this is impossible. So a value close to 1 is close enough. Achieving this is mostly dependent on high resolution compared to calculations over a large span.

To get a good visualization a high resolution is preferable because it will give more accurate details in the curves, thus the analytical expressions is best for visualization. The strength of the scatter diagram results is that it is easy to see if they are correct or not because it is a limited number of waves, and it is easy to understand what numbers to expect. Therefore these numbers can be used to compare and confirm the analytical expressions, which is done in the previous chapters.

The joint pdf of wave power and wave height gives an distribution where the wave power is seen to resemble a quadratic increase with the wave height, as it should by theory. For the joint pdf of wave power and wave period the shape is not so clear intuitively. The joint pdf of significant wave height and spectral peak period varies around the peak at $H_s = 2m$ and $T_p = 8s$.

For the long-term joint pdf of wave power and either wave height or wave period it is at first glance seen that the shape resembles what was seen for the short-term individual waves statistics. However the long-term statistics is much more concentrated for low wave energy, with much steeper contour lines.

When the long-term statistics is weighted for wave power the contours become less steep because higher values of wave power become more important. But the difference is not very big and it is still the waves with the lowest wave energy that gives the largest contribution. The biggest difference is for higher values of wave period and low wave energy where the contours will bend inward because the energy is very small.

For the long-term marginal pdf of wave power it is seen that the graph is very steep with a shape that resembles an exponential distribution, but it does not fit perfectly. Two different equations have been tested to find a suggestion in how the wave power varies, but none of them gives sufficiently good results to conclude with a analytical expressions for the long-term marginal pdf of wave power.

The cumulative distribution function of wave power is very steep and most of the waves, as for the marginal pdf of wave power, are located for low wave energy. However for the cdf it is easier to see the difference between the results calculated from analytical expressions and results from scatter diagram results.

For the different control systems it is seen that the methods using reactive loading gives the highest energy output because these methods gives the motion closest to optimal phase and amplitude. But they also use some energy in order to control the motion, and need complex calculations in order to predict the future values that they are dependent on. Therefore the resistive methods represented by latching and clutching still can be competitive even though they generally gives less power output, because they does not use energy in the controlling. Another advantage is that they give less peak-to-average ratios, so that the dimensions of the control mechanisms do not need to be as large.

When looking at the power absorption for different WEC's is it seen that the results is very dependent on the width of influence that are chosen. Preferably more information about this parameter should have been known, but it was not available. Another thing that will influence the results significantly is the values that are approximately redrawn from the original source, which have a lot of uncertainties. As mentioned it is especially at low values for power absorption that the

uncertainties are large. When that is put together with the knowledge that most of the waves in a long-term perspective have very low wave energy it is obvious that these large uncertainties also will apply for the long-term statistics. This will give the differences between the WEC's and the actual results limited interest, but the general trends are worth some attention.

The results show that most of the WEC's have an optimal value for the wave period where both the power absorption and the efficiency are at its largest. For the wave height the WEC's give largest power absorption for large values, but are most efficient for small wave heights.

When looking at the long-term results for power absorption it is difficult to see any clear differences for different wave heights and wave periods. But the differences in total integrated area are large. As the heaving buoy only absorbs 11% of the energy in the waves, the heaving two bodies system absorbs 30% and the pitching device and the floating OWC absorbs 45%. From the long-term marginal pdf of wave power and the long-term cdf of wave power it is seen that most of the difference in absorption is for low values of wave power. Because of the large assumed uncertainties of low values for wave power also the variation when those values are isolated are of interest. This give very similar results, with the heaving buoy as the poorest, but the floating OWC seems to be more efficient than the competitors when the wave energy becomes large.

7.2 Recommendations for further work

One thing that could be given more attention is the area where most of the waves occur where the wave energy is very low, by doing the calculations over only this area with a large resolution. Because so large portion of the waves occur in this area it would be interesting to investigate if there are any differences to notice.

Analytical expressions was attempted to be determined for the long-term pdf of wave power with lack of success. This could be investigated further in a more thoroughly way. Also analytical expressions for the long-term cdf of wave power would be interesting to find.

When looking at power absorption it would be interesting to implement the mentioned control mechanisms in the statistics, to see how they would influence the results in the long-term statistics.

References

[1] Aurelien Babarit, Jorgen Hals, Adi Kurniawan, Torgeir Moan, and Jorgen Krokstad. Power absorption measures and comparisons of selected wave energy converters. *ASME Conference Proceedings*, 2011(44373):437–446, 2011.

[2] Hagerman. Wave power. In New York: Wiley, editor, *Encyclopedia of energy technology and the environment*, pages 2859–907, 1995.

[3] Jørgen Hals. *Modelling and phase control of wave-energy converters.* PhD thesis, NTNU, May 2010.

[4] Jørgen Hals, Johannes Falnes, and Torgeir Moan. A comparison of selected strategies for adaptive control of wave energy converters. *Journal of Offshore Mechanics and Arctic Engineering*, 133(3):031101, 2011.

[5] Amir H. Izadparast and John M. Niedzwecki. Estimating the potential of ocean wave power resources. *Ocean Engineering*, 38(1):177 – 185, 2011.

[6] Michael E. McCormick. *Ocean Wave Energy Conversion.* Dover Publications, 1981.

[7] Dag Myrhaug, Bernt J. Leira, and Havard Holm. Wave power statistics for sea states. *Journal of Offshore Mechanics and Arctic Engineering*, 133(4):044501, 2011.

[8] Dag Myrhaug, Bernt J. Leira, and Havard Holm. Long term wave power statistics for individual waves. Unpublished draft, 2012.

[9] Dag Myrhaug, Bernt J. Leira, and Håvard Holm. Wave power statistics for individual waves. *Applied Ocean Research*, 31(4):246 – 250, 2009.

[10] Vengatesan Venugopal and George H. Smith. The effect of wave period filtering on wave power extraction and device tuning. *Ocean Engineering*, 34(8–9):1120 – 1137, 2007.

Appendices

Appendix A

Wave scatter diagram

A.1 For sea states

Frequency table for H_{m0} and T_p from Haltenbanken 1980-1985

H_{m0} \ T_p	<4	4-5	5-6	6-7	7-8	8-9	9-10	10-11	11-12	12-13	13-14	14-15	15-16	16-17	17-18	18-19	19-20	20-21	21-22	22 <	Sum
0.0-0.5	0	0	3	1	1	1	2	3	1	0	0	0	2	2		1					12
0.5-1.0	32	54	106	159	153	139	90	60	34	11	11	3	2	2		1	1				858
1.0-1.5	7	128	219	270	374	302	203	152	94	44	25	13	7	3	3	1			1		1846
1.5-2.0	0	20	182	268	307	378	261	184	94	85	46	18	8	9	2		1	1	1	2	1867
2.0-2.5		0	71	212	283	314	272	204	114	88	50	55	30	7	2	1	1	1	1	1	1707
2.5-3.0			10	105	183	221	191	155	146	95	64	45	14	7	1	2	2	2			1243
3.0-3.5				33	112	160	156	141	123	75	47	30	25	19	10	1	1				933
3.5-4.0				9	60	109	101	121	107	88	45	24	20	9	7	4					704
4.0-4.5				4	19	74	103	101	99	82	46	43	13	4	3	3			1		595
4.5-5.0					8	28	65	73	69	50	42	19	16	14	8	3					395
5.0-5.5					1	18	38	71	63	50	29	16	14	10	6	5					321
5.5-6.0						4	14	33	48	40	28	16	14	7	2	2					208
6.0-6.5						3	8	26	43	33	34	10	6	2	2						167
6.5-7.0								10	22	29	25	12	7	4	2						111
7.0-7.5								5	19	29	15	15	6	2	1	2					94
7.5-8.0								1	9	28	7	6	3	1	1						55
8.0-8.5								1	8	15	11	6	7	1	1						50
8.5-9.0									4	8	6	8	2	2		2					32
9.0-9.5									1	1	10	3	2	1							18
9.5-10.0										1	1	1	3	1	2	1					10
10.0-10.5											1	2	4	1	1						7
10.5-11.0										1			3	1	1		1				7
11.0-11.5												1	2		1						4
11.5-12.0														1							1
12<																					1
Sum	39	202	591	1061	1501	1751	1504	1341	1098	853	542	346	208	108	55	28	7	4	4	3	11246

A.2 For individual waves

T/√Hrms / Hrms	.05	.15	.25	.35	.45	.55	.65	.75	.85	.95	1.05	1.15	1.25	1.35	1.45	1.55	1.65	1.75	1.85	
.1		6	23	20	13	3	2													67
.3		1	42	114	132	98	48	33	11	3	3	2		1						488
.5		2	4	53	142	198	169	135	97	67	43	16	14	8	2	2				952
.7			1	12	54	127	171	159	170	132	121	67	56	29	17	5	3	2		1026
.9					12	57	107	121	162	182	149	143	97	62	24	8	2		1	1137
1.1					1	21	49	79	135	173	194	172	96	33	28	7	3	1	2	994
1.3						7	15	42	93	133	182	152	73	40	14	4	3			758
1.5							11	26	46	86	108	85	47	20	9	1	1		1	441
1.7						1	5	7	18	52	61	40	17	5	2					208
1.9							1	4	13	23	20	27	9	6						113
2.1								3	3	7	20	7	4		1					45
2.3								1	5	1	3	4	2							16
2.5										1	2	4								7
2.7																				
2.9												1								1

Appendix B

Matlab script used for the calculations

B.1 mainprog.m

Puts together the calculations for the long-term distributions. Three pre calculated examples are available for this run, because of the long calculation times (*lowreslargespan.mat*, *lowres.mat* and *highres.mat)*.

```
clear all
tttt = cputime; %calculates calculation time

%% inputvalues
listsandvalues; % makes alle the necessary lists, and some basic values
[B Hss Tps delHss delTps]=haltenbanken(); %put in wave scatter ...
    values for seastates
blist=individualwaves(); %put in wave scatter values for individual ...
    waves
[Hsb delHsb Tpb delTpb totpow hb effhb htbs effhtbs pd effpd fowc ...
    efffowc]=barbar(); %put in wave absorption matrices

%% Calculation of PL(J,X)
for i=1:length(J)
    for j=1:Xl
        %% PL(J,X)=int int p(J,X|Hs,Tp)p(Hs,Tp)w(Hs,Tz)dHsdTp
        % Long-term pdf from scatter
        [SL_JH(i,j) SL_JT(i,j)]=scatter(J(i), delJ, H(j), delH, ...
            T(j), delT, Hss, delHss, Tps, delTps, blist, B, gamma, g);
        J_SL_JH(i,j)=SL_JH(i,j)*J(i);
        J_SL_JT(i,j)=SL_JT(i,j)*J(i);

```

```
19          % Long-term pdf from analytical expressions
20          [PL_JH(i,j) PL_JT(i,j)]=formel(J(i), H(j), T(j), Hs, delHs, ...
                Tp, delTp, gamma, g);
21          J_PL_JH(i,j)=PL_JH(i,j)*J(i);
22          J_PL_JT(i,j)=PL_JT(i,j)*J(i);
23
24          % Long-term efficiency from scatter
25          [effhbL_JH(i,j) effhbL_JT(i,j)]= sceff(effhb, J(i), delJ, ...
                H(j), delH, T(j), delT, Hsb+0.25, delHsb, Tpb+0.5, ...
                delTpb, blist, B, gamma, g);
26          [effhtbsL_JH(i,j) effhtbsL_JT(i,j)]= sceff(effhtbs, J(i), ...
                delJ, H(j), delH, T(j), delT, Hsb+0.25, delHsb, ...
                Tpb+0.5, delTpb, blist, B, gamma ,g);
27          [effpdL_JH(i,j) effpdL_JT(i,j)]= sceff(effpd, J(i), delJ, ...
                H(j), delH, T(j), delT, Hsb+0.25, delHsb, Tpb, ...
                delTpb+0.5, blist, B, gamma, g);
28          [efffowcL_JH(i,j) efffowcL_JT(i,j)]= sceff(efffowc, J(i), ...
                delJ, H(j), delH, T(j), delT, Hsb+0.25, delHsb, ...
                Tpb+0.5, delTpb, blist, B, gamma, g);
29
30      end
31      home
32      disp(['cputime: ' num2str(floor(cputime-tttt)) 's']) ;
33      disp(['progress: ' num2str(floor(100* (i/length(J)))) ' %']);
34  end
35
36  % Long-term pdf from scatter
37  SLJH=SL_JH*(10^6);
38  SLJT=SL_JT*(10^6);
39  J_SLJH=J_SL_JH*(10^6);
40  J_SLJT=J_SL_JT*(10^6);
41
42  % Long-term pdf from analytical expressions
43  PLJH=PL_JH*(10^6);
44  PLJT=PL_JT*(10^6);
45  J_PLJH=J_PL_JH*(10^6);
46  J_PLJT=J_PL_JT*(10^6);
47
48  % Long-term efficiency from scatter
49  effhbL_JH = effhbL_JH *(10^6);
50  effhbL_JT = effhbL_JT *(10^6);
51  effhtbsL_JH = effhtbsL_JH *(10^6);
52  effhtbsL_JT = effhtbsL_JT *(10^6);
53  effpdL_JH = effpdL_JH *(10^6);
54  effpdL_JT = effpdL_JT *(10^6);
55  efffowcL_JH = efffowcL_JH *(10^6);
56  efffowcL_JT = efffowcL_JT *(10^6);
57
58  results; %presents some results
59  plotfunc; % plot
60  %cumulative; % plot and cdf calculations
61  %fittedcurve; % must run cumulative for this to work
62
63  disp(['total cputime: ' num2str((cputime-tttt)/60) 'min']); %total ...
        calculation times
```

B.1.1 listsandvalues.m

Defines neccessary lists and values.

```
1
2  %% General values
3  gamma= 1025; %[kg/m^3] fluid density
4  g=9.81; %[m/s^2] acceleration due to gravity
5
6  %% Lists for J, H and T
7
8  % % To include all the waves
9  % delJ= 400000;
10 % J=0+delJ/2:delJ:16000000;
11 % delH=0.5;
12 % H=0+delH/2:delH:40;
13 % delT=1.0;
14 % T=0+delT/2:delT:80;
15
16 % % Include only the important areas
17 % delJ= 100000;
18 % J=0+delJ/2:delJ:3000000;
19 % delH=0.25;
20 % H=0+delH/2:delH:20;
21 % delT=0.5;
22 % T=0+delT/2:delT:40;
23
24 % Very fine mesh
25 delJ= 10000;
26 J=0+delJ/2:delJ:3000000;
27 delH=0.025;
28 H=0+delH/2:delH:20;
29 delT=0.05;
30 T=0+delT/2:delT:40;
31
32 if length(H) ~= length(T) %makes sure H and T have equal lenghts
33     error('H and T must have equal lengths')
34 end
35
36 %% Lists for formula calculations
37 delHs=0.5;
38 Hs=0+delHs/2:delHs:12.5+delHs/2;
39
40 delTp=1.0;
41 Tp= 4+delTp/2:delTp:22+delTp/2;
42
43 %% Size of J,X matrix, output matrix
44 Xl=length(H); % length of the H and T table
45 %for scatter
46 SL_JH=zeros(length(J),Xl);
47 SL_JT=zeros(length(J),Xl);
48 J_SL_JH=zeros(length(J),Xl);
49 J_SL_JT=zeros(length(J),Xl);
50
51 %for smoothed curves
```

```
PL_JH=zeros(length(J),Xl);
PL_JT=zeros(length(J),Xl);
J_PL_JH=zeros(length(J),Xl);
J_PL_JT=zeros(length(J),Xl);

%for efficiency results
effhbL_JH = zeros(length(J),Xl);
effhbL_JT = zeros(length(J),Xl);
effhtbsL_JH = zeros(length(J),Xl);
effhtbsL_JT = zeros(length(J),Xl);
effpdL_JH = zeros(length(J),Xl);
effpdL_JT = zeros(length(J),Xl);
efffowcL_JH = zeros(length(J),Xl);
efffowcL_JT = zeros(length(J),Xl);
```

B.1.2 haltenbanken.m

Defines the values for the Haltenbanken wave scatter diagram given in appendix A.1.

```
function [B Hss Tps delHss delTps]=haltenbanken()

% The wave scatter
B=[
  0   0   3   1   1   1   2   3   1  0  0  0  0  0  0 0 0 0 0 0;
 32  54 106 159 153 139  90  60  34 11 11  3  2  2  0 1 1 0 0 0;
  7 128 219 270 374 302 203 152  94 44 25 13  7  3  3 1 0 0 1 0;
  0  20 182 268 307 378 261 184  94 85 46 18  8  9  2 0 1 1 1 2;
  0   0  71 212 283 314 272 204 114 88 50 55 30  7  2 1 1 1 1 1;
  0   0  10 105 183 221 191 155 146 95 64 45 14  7  1 2 2 2 0 0;
  0   0   0  33 112 160 156 141 123 75 47 30 25 19 10 1 1 0 0 0;
  0   0   0   9  60 109 101 121 107 88 45 24 20  9  7 4 0 0 0 0;
  0   0   0   4  19  74 103 101  99 82 46 43 13  4  3 3 0 0 1 0;
  0   0   0   0   8  28  65  73  69 50 42 19 16 14  8 3 0 0 0 0;
  0   0   0   0   1  18  38  71  63 50 29 16 14 10  6 5 0 0 0 0;
  0   0   0   0   0   4  14  33  48 40 28 16 14  7  2 2 0 0 0 0;
  0   0   0   0   0   3   8  26  43 33 34 10  6  2  2 0 0 0 0 0;
  0   0   0   0   0   0   0  10  22 29 25 12  7  4  2 0 0 0 0 0;
  0   0   0   0   0   0   0   5  19 29 15 15  6  2  1 2 0 0 0 0;
  0   0   0   0   0   0   0   1   9 28  7  6  3  1  0 0 0 0 0 0;
  0   0   0   0   0   0   0   1   8 15 11  6  7  1  1 0 0 0 0 0;
  0   0   0   0   0   0   0   0   4  8  6  8  2  2  0 2 0 0 0 0;
  0   0   0   0   0   0   0   0   1  1 10  3  2  1  0 0 0 0 0 0;
  0   0   0   0   0   0   0   0   0  1  1  1  3  1  2 1 0 0 0 0;
  0   0   0   0   0   0   0   0   0  0  0  2  4  0  1 0 0 0 0 0;
  0   0   0   0   0   0   0   0   0  1  0  0  3  1  1 0 1 0 0 0;
  0   0   0   0   0   0   0   0   0  0  0  1  2  0  1 0 0 0 0 0;
  0   0   0   0   0   0   0   0   0  0  0  0  0  1  0 0 0 0 0 0;
  0   0   0   0   0   0   0   0   0  0  0  0  0  1  0 0 0 0 0 0];

% Signigicant wave heights
Hss=[
```

```
0.00000001  0.5 0.25;
0.5  1.0    0.75;
1.0  1.5    1.25;
1.5  2.0    1.75;
2.0  2.5    2.25;
2.5  3.0    2.75;
3.0  3.5    3.25;
3.5  4.0    3.75;
4.0  4.5    4.25;
4.5  5.0    4.75;
5.0  5.5    5.25;
5.5  6.0    5.75;
6.0  6.5    6.25;
6.5  7.0    6.75;
7.0  7.5    7.25;
7.5  8.0    7.75;
8.0  8.5    8.25;
8.5  9.0    8.75;
9.0  9.5    9.25;
9.5  10.0   9.75;
10.0 10.5  10.25;
10.5 11.0  10.75;
11.0 11.5  11.25;
11.5 12.0  11.75;
12.0 12.5  12.25];

% Spectral peak periods
Tps=[
3.0 4.0 5.0 6.0 7.0 8.0  9.0    10.0    11.0    12.0    13.0    ...
    14.0    15.0    16.0    17.0    18.0    19.0    20.0    ...
    21.0    22.0;
4.0 5.0 6.0 7.0 8.0 9.0 10.0    11.0    12.0    13.0    14.0    ...
    15.0    16.0    17.0    18.0    19.0    20.0    21.0    ...
    22.0    23.0;
3.5 4.5 5.5 6.5 7.5 8.5  9.5    10.5    11.5    12.5    13.5    ...
    14.5    15.5    16.5    17.5    18.5    19.5    20.5    ...
    21.5    22.5];

%% Lists for scatter calculations
delHss=Hss(1,2)-Hss(1,1);

delTps=Tps(2,1)-Tps(1,1);

end %function
```

B.1.3 individualwaves.m

Defines the values for the Individual wave scatter diagram given in appendix A.2.

```
function blist=individualwaves()

% reads in necessary values to do the calculations
```

```
4
5  %% Wave scatter (MK84)
6  b=[
7  0   6   23  20  13  3   2   0   0   0   0   0   0   0   0   0   ...
       0   0;
8  0   1   42  114 132 98  48  33  11  3   3   2   0   1   0   0   0   ...
       0   0;
9  0   2   4   53  142 198 169 135 97  67  43  16  14  8   2   2   0   ...
       0   0;
10 0   0   1   12  54  127 171 159 170 132 121 67  56  29  17  5   3   ...
       2   0;
11 0   0   0   0   12  57  107 121 162 192 149 143 97  62  24  8   2   ...
       0   1;
12 0   0   0   0   1   21  49  79  135 173 194 172 96  33  28  7   3   ...
       1   2;
13 0   0   0   0   0   7   15  42  93  133 182 152 73  40  14  4   3   ...
       0   0;
14 0   0   0   0   0   0   11  26  46  86  108 85  47  20  9   1   1   ...
       0   1;
15 0   0   0   0   0   1   5   7   18  52  61  40  17  5   2   0   0   ...
       0   0;
16 0   0   0   0   0   0   1   4   13  23  30  27  9   6   0   0   0   ...
       0   0;
17 0   0   0   0   0   0   0   3   3   7   20  7   4   0   1   0   0   ...
       0   0;
18 0   0   0   0   0   0   0   1   5   1   3   4   2   0   0   0   0   ...
       0   0;
19 0   0   0   0   0   0   0   0   0   1   2   4   0   0   0   0   0   ...
       0   0;
20 0   0   0   0   0   0   0   0   0   0   0   0   0   0   0   0   0   ...
       0   0;
21 0   0   0   0   0   0   0   0   0   0   0   1   0   0   0   0   0   ...
       0   0];
22
23 % t=T/Trms
24 t=[0.05 0.15    0.25    0.35    0.45    0.55    0.65    0.75    ...
       0.85    0.95    1.05    1.15    1.25    1.35    1.45    ...
       1.55    1.65    1.75    1.85];
25 delt= t(2)-t(1);
26
27 % h=H/Hrms
28 h=[0.1;0.3;0.5;0.7;0.9;1.1;1.3;1.5;1.7;1.9;2.1;2.3;2.5;2.7;2.9];
29 delh=h(2)-h(1);
30
31 % Rewrite the scatter to a list
32 blist=zeros(sum(sum(b)),4);
33 bnum=0;
34
35 for i=1:length(h)
36     for j=1:length(t)
37         n=b(i,j);
38
39         while n>0
40             nr=floor(sqrt(n)); % n root value
41             dh=delh/nr; % h step
42             dt=delt/nr; % t step
43             for k = 1:nr
```

```
                    for m=1:nr
                        bnum=bnum+1;
                        hi=h(i)-(delh/2)+(k-0.5)*dh; % h value
                        ti=t(j)-(delt/2)+(m-0.5)*dt; % t value
                        ji=(hi^2)*ti; % j value
                        blist(bnum,:)=[bnum hi ti ji]; % put it in the list
                    end
                end
                n=n-(nr^2);
            end
        end
    end
end %function
```

B.1.4 barbar.m

Defines the power matrices from [1], and calculates the efficiency.

```
function [Hsb delHsb Tpb delTpb totpow hb effhb htbs effhtbs pd ...
    effpd fowc efffowc]=barbar()

% Hs values
Hsb =[ 0.5 1 1.5 2 2.5 3 3.5 4 4.5 5 5.5 6 6.5 7 7.5];

% Tp values
Tpb = [3 4 5 6 7 8 9 10 11 12 13 14 15 16 17];

% Interval sizes
delHsb=Hsb(2)-Hsb(1);
delTpb=Tpb(2)-Tpb(1);

%% Total available power
gamma=1025;
g=9.81;
alpha=0.91; %for Tp
fak=gamma*(g^2)/(64*pi*1000)*alpha; %factor

totpow=zeros(length(Hsb),length(Tpb));

for i=1:length(Hsb)
    for j=1:length(Tpb)
        totpow(i,j)=(Hsb(i)^2)*Tpb(j)*fak;
    end
end

%% Power matrix of the heaving buoy [kW]
hb=[
0   0.2     0   0   0   0   0   0   0   0   0   0   0   0   0;
1   1.2   1.2 1.2 1.2 1.1   1   1 0.9 0.8 0.8 0.6 0.6 0.6 0.5;
0.5 2.5   2.5 2.3 2.2 2.2 2 1.9 1.7 1.5 1.5 1.3 1.2 1.2 1;
0.8 4 4   3.8 3.5 3.5 3.1 2.8 2.7 2.3 2.2 2 1.9 1.8 1.7;
0   0.8   6   5.1 4.7 4.6 4.2 3.9 3.5 3 2.8 2.6 2.7 2.6 2.4;
```

```
0   0.9 7.2 6.8 6.2 5.8 5.3 4.8 4.2 4.1 3.6 3.2 3.3 3.1 2.9;
0   0.9 9.2 8.3 7.3 6.8 5.9 5.4 4.9 4.6 4.2 3.8 3.7 3.6 3.3;
0   0.2 0.9 8.9 8.5 7.7 6.7 6.2 5.6 5 4.8 4.5 4.2 3.9 3.7;
0   0.2 0.9 10 9.6 8.6 7.8 7 6.2 5.8 5.3 5.1 4.9 4.4 4.1;
0   0.2 0.9 10.2 10.3 9.3 8.4 7.6 7.1 6.4 5.8 5.6 5.4 5 5;
0   0.2 0.9 10.1 10.5 10.1 8.9 8.1 7.5 6.8 6.4 6.1 5.7 5.5 5.3;
0   0 0.2 0.9 10.2 10.6 10 9.1 8.3 7.5 6.8 6.9 6.3 5.8 5.6;
0   0 0.2 0.9 10.2 10.8 10.5 9.7 9 7.8 7.5 7.3 6.7 6.3 5.8;
0   0 0.2 0.9 10.3 10.9 10.8 10 8.9 8.3 8.1 7.6 7.2 6.8 6.2;
0   0 0.2 0.9 10.4 10.9 10.9 10.5 10 8.8 8.4 7.8 7.5 7.1 6.5];

dhb=1.5; %[m] width of influence
effhb=hb./(totpow*dhb);

%% Power matrix of the heaving two bodies system [kW]
htbs=[
0 0 0 0 0 0 0 0 0 0 0 0 0 0;
0 0 0 0 0 20 50 50 20 0 0 0 0 0 0;
0 0 0 20 50 80 90 110 110 90 80 50 20 0 0;
0 0 20 60 90 120 140 190 170 140 120 100 60 50 0;
0 20 60 110 150 170 190 270 240 210 180 150 110 90 50;
0 40 90 150 200 230 290 370 310 310 250 180 160 130 100;
0 50 110 190 280 340 420 480 410 370 330 260 210 170 140;
0 40 80 240 350 420 520 600 480 430 390 290 240 180 170;
0 20 90 300 420 570 630 590 650 610 480 370 290 250 210;
0 20 90 360 500 710 760 790 730 590 570 420 360 310 250;
0 20 90 400 620 770 900 900 790 760 700 500 380 400 280;
0 0 30 90 720 870 930 930 920 910 730 570 470 420 350;
0 0 30 90 810 920 950 960 950 920 780 640 490 470 430;
0 0 30 90 840 940 960 970 960 950 920 770 680 570 470;
0 0 30 90 900 950 970 980 960 920 790 900 730 620 530];

dhtbs=20; %[m] width of influence
effhtbs=htbs./(totpow*dhtbs);

%% Power matrix of the pitching device [kW]

pd=[
0 0 0 10 20 30 20 10 0 0 0 0 0 0 0;
0 0 40 60 80 90 70 40 0 0 0 0 0 0 0;
0 50 80 120 180 170 130 90 60 20 0 0 0 0 0;
0 80 130 190 290 270 190 150 100 70 20 0 0 0 0;
0 60 190 290 420 390 310 200 160 120 70 50 20 0 0;
0 80 260 390 480 500 390 280 210 170 110 110 70 40 0;
0 90 340 560 760 740 490 380 280 220 160 140 120 70 20;
0 30 90 730 920 850 620 470 350 270 190 170 140 90 60;
0 20 90 900 1020 1010 780 600 390 320 200 220 180 130 110;
0 20 90 1010 1030 1020 880 660 460 370 310 260 220 170 130;
0 20 90 1010 1040 1040 1010 780 580 440 370 280 240 180 160;
0 0 40 90 1020 1050 1030 1000 670 530 420 330 270 210 180;
0 0 20 90 1020 1060 1040 1000 700 610 470 370 280 240 210;
0 0 20 90 1020 1070 1060 1020 880 680 490 420 300 310 250;
0 0 20 90 1030 1080 1070 1040 970 600 520 440 350 300 270];

dpd=25; %[m] width of influence
effpd=pd./(totpow*dpd);

```

```
91  %% Power matrix of the floating OWC
92
93  fowc=[
94  0 0 0 0 0 10 10 10 0 0 0 0 0 0 0;
95  0 0 0 20 50 70 70 60 50 40 40 40 30 10 0;
96  0 0 20 60 100 130 140 120 100 90 90 90 90 70 40;
97  0 20 60 110 180 230 240 210 180 170 160 170 160 130 90;
98  10 60 110 180 280 360 380 320 280 260 250 250 230 190 150;
99  30 80 160 260 380 500 510 480 400 370 360 370 350 280 200;
100 50 90 210 340 530 680 720 640 540 490 480 490 470 370 280;
101 70 130 280 430 680 890 940 830 700 640 620 640 600 480 370;
102 80 180 370 570 850 1010 1020 1010 900 800 780 790 760 600 470;
103 90 200 430 680 1010 1030 1030 1020 1010 990 970 990 950 760 580;
104 100 250 510 830 1020 1040 1040 1040 1030 1020 1020 1020 1010 800 690;
105 110 290 620 990 1020 1050 1050 1050 1040 1030 1030 1030 1020 1010 810;
106 150 320 750 1010 1030 1050 1060 1060 1050 1040 1040 1040 1030 1020 960;
107 170 390 840 1020 1040 1060 1070 1070 1060 1050 1050 1050 1040 1030 ...
        1020;
108 190 420 960 1030 1050 1070 1080 1080 1070 1060 1060 1060 1050 1040 ...
        1030];
109
110 dfowc=24; %[m] width of influence
111 efffowc=fowc./(totpow*dfowc);
```

B.1.5 scatter.m

Calculates the long-term distribution from equation 3.8 by using the wave scatter diagram values.

```
1   function [SL_JH SL_JT]=scatter(J,delJ,H,delH,T,delT,Hss,delHss,Tps, ...
        delTps,blist,B,gamma,g)
2
3   s_JH=zeros(length(Hss),length(Tps));
4   s_JT=zeros(length(Hss),length(Tps));
5   s_HssTps=zeros(length(Hss),length(Tps));
6
7   J1=J-delJ/2;
8   J2=J+delJ/2;
9   H1=H-delH/2;
10  H2=H+delH/2;
11  T1=T-delT/2;
12  T2=T+delT/2;
13
14  for m=1:length(Hss)
15
16      Hrms  = 0.714 * Hss(m,3);
17
18      for n=1:length(Tps)
19          if B(m,n)>0 %for increasing speed
20              Trms  = 0.97 * Tps(3,n);
21
22              Jch  = gamma *(g^2) * (Hrms^2) * Trms/(32*pi); % Jchar
```

```
23
24              bjh=0;
25              bjt=0;
26              for o=1:length(blist)
27                  bH = blist(o,2)*Hrms;
28                  bT = blist(o,3)*Trms;
29                  bJ = blist(o,4)*Jch;
30
31                  if bJ >= J1 && bJ < J2 % if j-value is in the interval
32                      if bH >= H1 && bH < H2 % if h-value is in the ...
                            interval
33                          bjh=bjh+1;
34                      end
35                      if bT >= T1 && bT < T2 % if t-value is in the ...
                            interval
36                          bjt=bjt+1;
37                      end
38                  end
39              end
40
41              %% J and H
42              s_jh=bjh/length(blist);
43              s_JH(m,n) = s_jh / (delH * delJ);
44
45              %% J and T
46              s_jt=bjt/length(blist);
47              s_JT(m,n) = s_jt / (delT * delJ);
48
49              %% Hs and Tp
50              s_HssTps(m,n) = B(m,n)/sum(sum(B))/(delHss*delTps);
51          end
52      end
53  end
54
55  %% w(Hs,Tchar)
56  w_HssTzs=1;
57
58  %% Return values
59  int_JHs = s_JH .* s_HssTps .* w_HssTzs;
60  int_JTs = s_JT .* s_HssTps .* w_HssTzs;
61
62  SL_JH = sum(sum(int_JHs)) * delHss * delTps;
63  SL_JT = sum(sum(int_JTs)) * delHss * delTps;
64
65  end %function
```

B.1.6 formel.m

Calculates the long-term distribution from equation 3.3 by using the analytical values given in appendix B.1.7, B.1.8, B.1.9, B.1.10, B.1.11 and B.1.12.

```
1  function [PL_JH PL_JT]=formel(J,H,T,Hs,delHs,Tp,delTp,gamma,g)
```

```
2
3  p_JH=zeros(length(Hs),length(Tp));
4  p_JT=zeros(length(Hs),length(Tp));
5  p_HsTp=zeros(length(Hs),length(Tp));
6  Tplist=zeros(length(Hs),length(Tp));
7
8  for m=1:length(Hs)
9
10     Hrms=0.714 * Hs(m);
11     h=H/Hrms; % Dimentionless wave height
12
13     for n=1:length(Tp)
14
15         Trms=0.97 * Tp(n);
16         t=T/Trms; % Dimentionless wave period
17
18         Jch= gamma *(g^2) * (Hrms^2) * Trms/(32*pi); % Jchar
19         jj=J/Jch; % Dimentionless wave energy
20
21         %% J and H
22         p_jgh= fp_jgh(h,jj);
23         p_h  = fp_h(h);
24         p_jh  = p_jgh * p_h;
25
26         p_JH(m,n) = p_jh *32*pi/(gamma *(g^2) * (Hrms^3) * Trms);
27
28         %% J and T
29         p_jkt = fp_jkt (t,jj );
30         p_tgj = fp_tgj (t,jj );
31         p_jt  = p_tgj*p_jkt;
32
33         p_JT(m,n) = p_jt *32*pi/(gamma *(g^2) * (Hrms^2) * (Trms^2));
34
35         %% Hs and Tp
36         p_TpgHs = fp_TpgHs (Hs(m), Tp(n));
37         p_Hs = fp_Hs (Hs(m));
38         p_HsTp(m,n) = p_TpgHs * p_Hs;
39
40         %% Table of Tp-values
41         Tplist(m,n)=Tp(n);
42     end
43 end
44
45 %% w(Hs,Tchar)
46 meanTch=fmeanTch(Hs,delHs);
47 w_HsTz=meanTch ./ Tplist;
48
49 int_JH = p_JH .* p_HsTp .* w_HsTz;
50 int_JT = p_JT .* p_HsTp .* w_HsTz;
51
52 PL_JH = sum(sum(int_JH)) * delHs * delTp;
53 PL_JT = sum(sum(int_JT)) * delHs * delTp;
54
55 end %function
```

B.1.7 fp_ h.m

Calculates the marginal pdf of h given in equation 2.12.

```
function p_h=fp_h(h)
% calculates p(h)
p_h= ((2.39*h^1.39)/(1.05^2.39))*exp(-(h/1.05)^2.39);
end
```

B.1.8 fp_ jgh.m

Calculates the conditional pdf of j given h, given in equation 2.13.

```
function p_jgh = fp_jgh(h,jj )
% calculates p(j|h)

alfa=0.12* sqrt(h);

if h<=0.9
    rho=0.78*h+0.26;
else
    rho=0.962;
end

beta= 2*atan(2*(h-1.2))+5;

if jj>=alfa*h^2 && h>0
    p_jgh=(beta/(rho*h^2)) *(((jj-alfa*h^2)/(rho*h^2))^(beta-1)) ...
        *exp(-(((jj-alfa*h^2)/(rho*h^2))^(beta)));
else
    p_jgh=0;
end

end %function
```

B.1.9 fp_ jkt.m

Calculates the marginal pdf of j which is dependent on t, given in equation 2.18.

```
function p_jkt = fp_jkt(t,jj )
% calculates p(j;t) with averaging to discrete values

r=(1.05^2)*t;
s=2.39/2;
```

```
6
7  %p(j;t) , for j>=0
8  if jj>=0 && r>0
9      p_jkt=(s/r)*((jj/r)^(s-1))*exp(-(jj/r)^s);
10 else
11     p_jkt=0;
12 end
13
14 end %function
```

B.1.10 fp_ tgj.m.m

Calculates the conditional pdf of t given j, given in equation 2.21.

```
1  function p_tgj = fp_tgj(t,jj )
2  % calculates p(t|j)
3
4  h=sqrt(jj/t);
5
6  alfa=0.12* sqrt(h);
7
8  if h<=0.9
9      rho=0.78*h+0.26;
10 else
11     rho=0.962;
12 end
13
14 beta= 2*atan(2*(h-1.2))+5;
15
16 % p(t|h=sqrt(j/t))
17 if t>=alfa
18     p_tgj= (beta/rho) *(((t-alfa)/(rho))^(beta-1)) ...
           *exp(-(((t-alfa)/(rho))^(beta)));
19 else
20     p_tgj=0;
21 end
22
23 end %function
```

B.1.11 fp_ Hs.m

Calculating the marginal pdf of H_s, given in equation 2.24.

```
1  function p_Hs = fp_Hs (Hs)
2
3  if Hs <= 3.25 && Hs>0 % [m]
4      teta=0.801;
```

```
5       kap=sqrt(0.371);
6       p_Hs = (1/(sqrt(2*pi)*kap*Hs)) * ...
            exp(-((log(Hs)-teta)^2)/(2*kap^2));
7   else
8       zeta=2.713;
9       beta=1.531;
10      p_Hs = (beta*(Hs^(beta-1))/(zeta^beta)) * exp(-(Hs/zeta)^beta);
11  end
12
13  end %function
```

B.1.12 fp_ TpgHs.m

Calculating the conditional pdf of T_p given H_s, given in equation 2.25.

```
1   function p_TpgHs = fp_TpgHs (Hs, Tp)
2
3   a1=1.780;
4   a2=0.288;
5   a3=0.474;
6
7   b1=0.001;
8   b2=0.097;
9   b3=-0.255;
10
11  mu=a1 + a2*Hs^a3;
12  sigma=sqrt(b1 + b2*exp(b3*Hs));
13
14  if Tp>0 && Hs>0
15      p_TpgHs= (1/(sqrt(2*pi)*sigma*Tp)) * ...
            exp(-((log(Tp)-mu)^2)/(2*sigma^2));
16  else
17      p_TpgHs=0;
18  end
19
20  end %function
```

B.1.13 fmeanTch.m

Calculates the average wave period.

```
1   function meanTch=fmeanTch(Hs,delHs)
2
3   meanTch=0;
4
5   a1=1.780;
6   a2=0.288;
```

```
a3=0.474;

b1=0.001;
b2=0.097;
b3=-0.255;

for i = 1:length(Hs)
    mu=a1 + a2*Hs(i)^a3;
    sigma=sqrt(b1 + b2*exp(b3*Hs(i)));

    p_Hs= fp_Hs (Hs(i));

    meanTchint=exp(mu+0.5*sigma^2)*p_Hs;

    meanTch = meanTch + meanTchint*delHs;
end

end %function
```

B.1.14 sceff.m

Calculates the long-term distribution off power absorption from equation 6.1 by using the power matrices from barbar.m.

```
function [SL_JH ...
    SL_JT]=sceff(effmat,J,delJ,H,delH,T,delT,Hss,delHss,Tps, ...
    delTps,blist,B,gamma,g)

s_JH=zeros(length(Hss),length(Tps));
s_JT=zeros(length(Hss),length(Tps));
s_HssTps=zeros(length(Hss),length(Tps));

J1=J-delJ/2;
J2=J+delJ/2;
H1=H-delH/2;
H2=H+delH/2;
T1=T-delT/2;
T2=T+delT/2;

for m=1:length(Hss)

    Hrms  = 0.714 * Hss(m);

    for n=1:length(Tps)
        if B(m,n)>0 %for increasing speed
            Trms  = 0.97 * Tps(n);

            Jch  = gamma *(g^2) * (Hrms^2) * Trms/(32*pi); % Jchar

            bjh=0;
            bjt=0;
            for o=1:length(blist)
```

```
27                  bH = blist(o,2)*Hrms;
28                  bT = blist(o,3)*Trms;
29                  bJ = blist(o,4)*Jch;
30
31                  if bJ >= J1 && bJ < J2 % if j-value is in the interval
32                      if bH >= H1 && bH < H2 % if h-value is in the ...
                            interval
33                          bjh=bjh+1;
34                      end
35                      if bT >= T1 && bT < T2 % if t-value is in the ...
                            interval
36                          bjt=bjt+1;
37                      end
38                  end
39              end
40
41              %% J and H
42              s_jh=bjh/length(blist);
43              s_JH(m,n) = s_jh / (delH * delJ);
44
45              %% J and T
46              s_jt=bjt/length(blist);
47              s_JT(m,n) = s_jt / (delT * delJ);
48
49              %% Hs and Tp
50              s_HssTps(m,n) = B(m+1,n)/sum(sum(B))/(delHss*delTps);
51
52              %% adding in the efficiency
53              mp1=m+1;
54              np1=n+1;
55              if m+1>length(Hss)
56                  mp1=m;
57              end
58              if n+1>length(Tps)
59                  np1=n;
60              end
61              effvalue= (effmat(m,n) +effmat(mp1,n) + effmat(m,np1) + ...
                    effmat(mp1,np1) )/4;
62              s_HssTps(m,n)=s_HssTps(m,n) * effvalue;
63          end
64      end
65  end
66
67  %% w(Hs,Tchar)
68  w_HssTzs=1;
69
70  %% Return values
71  int_JHs = s_JH .* s_HssTps .* w_HssTzs;
72  int_JTs = s_JT .* s_HssTps .* w_HssTzs;
73
74  SL_JH = sum(sum(int_JHs)) * delHss * delTps;
75  SL_JT = sum(sum(int_JTs)) * delHss * delTps;
76
77  end %function
```

B.1.15 results.m

Presents some of the results from the calculations.

```
1
2  disp(['sum(SLJH)= ' num2str(sum(sum(SL_JH*delJ*delH)))]);
3  disp(['sum(SLJT)= ' num2str(sum(sum(SL_JT*delJ*delT)))]);
4  disp(['sum(PLJH)= ' num2str(sum(sum(PL_JH*delJ*delH)))]);
5  disp(['sum(PLJT)= ' num2str(sum(sum(PL_JT*delJ*delT)))]);
6
7  disp(['sum(SLJH) without start= ' ...
       num2str(sum(sum(SL_JH(:,7:80)*delJ*delH )))]);
8  disp(['sum(PLJH) without start= ' ...
       num2str(sum(sum(PL_JH(:,7:80)*delJ*delH )))]);
9
10 disp(['sum(effhbL_JH)= ' ...
       num2str(sum(sum(effhbL_JH*delJ*(10^-6)*delH)))]);
11 disp(['sum(effhbL_JT)= ' ...
       num2str(sum(sum(effhbL_JT*delJ*(10^-6)*delT)))]);
12 disp(['sum(effhtbsL_JH)= ' ...
       num2str(sum(sum(effhtbsL_JH*delJ*(10^-6)*delH)))]);
13 disp(['sum(effhtbsL_JT)= ' ...
       num2str(sum(sum(effhtbsL_JT*delJ*(10^-6)*delT)))]);
14 disp(['sum(effpdL_JH)= ' ...
       num2str(sum(sum(effpdL_JH*delJ*(10^-6)*delH)))]);
15 disp(['sum(effpdL_JT)= ' ...
       num2str(sum(sum(effpdL_JT*delJ*(10^-6)*delT)))]);
16 disp(['sum(efffowcL_JH)= ' ...
       num2str(sum(sum(efffowcL_JH*delJ*(10^-6)*delH)))]);
17 disp(['sum(efffowcL_JT)= ' ...
       num2str(sum(sum(efffowcL_JT*delJ*(10^-6)*delT)))]);
```

B.1.16 plotfunc.m

Makes the plots for the long-term distribution results.

```
1
2  %% scatter individual waves
3  figure
4  plot(blist(:,3),blist(:,2),'b.')
5  set(gca,'YDir','reverse')
6  xlabel('t')
7  ylabel('h')
8
9  %% ——————————   Scatter  ————————————————————
10 %% Plot SLJH and SLJT
11 % SLJH
12 figure
13 subplot(1,2,1)
```

```
14 contour(H,J*(10^-6),SLJH,[0.00001 0.0001 0.001 0.005 0.01 0.05 0.1 ...
       0.2])
15 title('P_L(J,H)')
16 xlabel('H[m]')
17 ylabel('J[MW]')
18
19 % SLJT
20 subplot(1,2,2)
21 contour(T,J*(10^-6),SLJT,[0.00001 0.0001 0.001 0.005 0.01 0.05 0.1 ...
       0.2])
22 title('P_L(J,T)')
23 xlabel('T[s]')
24 ylabel('J[MW]')
25
26 set(gcf, 'PaperType', 'B5')
27 set(gcf,'PaperUnits','centimeters','PaperPosition', [0.63, 0.63, ...
       15.0, 7.0]);
28 print(figure(2),'-dpsc','figure/ch1/sljx.eps')
29
30 %% Plot J_SLJH and J_SLJT
31 % J_SLJH
32 figure
33 subplot(1,2,1)
34 contour(H,J*(10^-6),J_SLJH*(10^-6),[0.00001 0.0001 0.001 0.005 0.01 ...
       0.05 0.1 0.2])
35 title('J \times P_L(J,H)')
36 xlabel('H[m]')
37 ylabel('J[MW]')
38
39 % J_SLJT
40 subplot(1,2,2)
41 contour(T,J*(10^-6),J_SLJT*(10^-6),[0.00001 0.0001 0.001 0.005 0.01 ...
       0.05 0.1 0.2])
42 title('J \times P_L(J,T)')
43 xlabel('T[s]')
44 ylabel('J[MW]')
45
46 set(gcf, 'PaperType', 'B5')
47 set(gcf,'PaperUnits','centimeters','PaperPosition', [0.63, 0.63, ...
       15.0, 7.0]);
48 print(figure(3),'-dpsc','figure/ch1/jsljx.eps')
49
50 %% ---------------  Smoothed curves -------------
51 %% Plot PLJH and PLJT
52 % PLJH
53 figure
54 subplot(1,2,1)
55 contour(H,J*(10^-6),PLJH,[0.00001 0.0001 0.001 0.005 0.01 0.05 0.1 ...
       0.2])
56 title('P_L(J,H)')
57 xlabel('H[m]')
58 ylabel('J[MW]')
59
60 % PLJT
61 subplot(1,2,2)
62 contour(T,J*(10^-6),PLJT,[0.00001 0.0001 0.001 0.005 0.01 0.05 0.1 ...
       0.2])
```

```
63  title('P_L(J,T)')
64  xlabel('T[s]')
65  ylabel('J[MW]')
66
67  set(gcf, 'PaperType', 'B5')
68  set(gcf,'PaperUnits','centimeters','PaperPosition', [0.63, 0.63, ...
        15.0, 7.0]);
69  print(figure(4),'-dpsc','figure/ch1/pljx.eps')
70
71  %% Plot J_PLJH and J_PLJT
72  % J_PLJH
73  figure
74  subplot(1,2,1)
75  contour(H,J*(10^-6),J_PLJH*(10^-6),[0.00001 0.0001 0.001 0.005 0.01 ...
        0.05 0.1 0.2])
76  title('J \times P_L(J,H)')
77  xlabel('H[m]')
78  ylabel('J[MW]')
79
80  % J_PLJT
81  subplot(1,2,2)
82  contour(T,J*(10^-6),J_PLJT*(10^-6),[0.00001 0.0001 0.001 0.005 0.01 ...
        0.05 0.1 0.2])
83  title('J \times P_L(J,T)')
84  xlabel('T[s]')
85  ylabel('J[MW]')
86
87  set(gcf, 'PaperType', 'B5')
88  set(gcf,'PaperUnits','centimeters','PaperPosition', [0.63, 0.63, ...
        15.0, 7.0]);
89  print(figure(5),'-dpsc','figure/ch1/jpljx.eps')
90
91
92  %% ------------  Efficiency  ----------------
93
94  %% Power matrix of the heaving buoy [kW]
95  figure
96  subplot(1,2,1)
97  contourf(Tpb,Hsb,hb)
98  title('Power absorption [kW]')
99  xlabel('T_p[s]')
100 ylabel('H_s[m]')
101 colorbar
102
103 subplot(1,2,2)
104 contourf(Tpb,Hsb,effhb)
105 title('Efficiency [%]')
106 xlabel('T_p[s]')
107 ylabel('H_s[m]')
108 colorbar
109
110 set(gcf, 'PaperType', 'B5')
111 set(gcf,'PaperUnits','centimeters','PaperPosition', [0.63, 0.63, ...
        15.0, 7.0]);
112 print(figure(6),'-dpsc','figure/ch3/hb.eps')
113
114 %% Power matrix of the heaving two bodies system [kW]
```

```
figure
subplot(1,2,1)
contourf(Tpb,Hsb,htbs)
title('Power absorption [kW]')
xlabel('T_p[s]')
ylabel('H_s[m]')
colorbar

subplot(1,2,2)
contourf(Tpb,Hsb,effhtbs)
title('Efficiency [%]')
xlabel('T_p[s]')
ylabel('H_s[m]')
colorbar

set(gcf, 'PaperType', 'B5')
set(gcf,'PaperUnits','centimeters','PaperPosition', [0.63, 0.63, ...
    15.0, 7.0]);
print(figure(7),'-dpsc','figure/ch3/htbs.eps')

%% Power matrix of the pitching device [kW]
figure
subplot(1,2,1)
contourf(Tpb,Hsb,pd)
title('Power absorption [kW]')
xlabel('T_p[s]')
ylabel('H_s[m]')
colorbar

subplot(1,2,2)
contourf(Tpb,Hsb,effpd)
title('Efficiency [%]')
xlabel('T_p[s]')
ylabel('H_s[m]')
colorbar

set(gcf, 'PaperType', 'B5')
set(gcf,'PaperUnits','centimeters','PaperPosition', [0.63, 0.63, ...
    15.0, 7.0]);
print(figure(8),'-dpsc','figure/ch3/pd.eps')

%% Power matrix of the floating OWC
figure
subplot(1,2,1)
contourf(Tpb,Hsb,fowc)
title('Power absorption [kW]')
xlabel('T_p[s]')
ylabel('H_s[m]')
colorbar

subplot(1,2,2)
contourf(Tpb,Hsb,efffowc)
title('Efficiency [%]')
xlabel('T_p[s]')
ylabel('H_s[m]')
colorbar

```

```
170 set(gcf, 'PaperType', 'B5')
171 set(gcf,'PaperUnits','centimeters','PaperPosition', [0.63, 0.63, ...
        15.0, 7.0]);
172 print(figure(9),'-dpsc','figure/ch3/fowc.eps')
173
174 %-----------------------------------
175 %% Efficiency matrix of the heaving buoy [kW]
176 figure
177 subplot(1,2,1)
178 contour(H,J*(10^-6),effhbL_JH,[0.00001 0.0001 0.001 0.005 0.01 0.05 ...
        0.1 0.2])
179 title('p_{L,\eta_{hb}}(J,H)')
180 xlabel('H[m]')
181 ylabel('J[MW]')
182
183 subplot(1,2,2)
184 contour(T,J*(10^-6),effhbL_JT,[0.00001 0.0001 0.001 0.005 0.01 0.05 ...
        0.1 0.2])
185 title('p_{L,\eta_{hb}}(J,T)')
186 xlabel('T[s]')
187 ylabel('J[MW]')
188
189 set(gcf, 'PaperType', 'B5')
190 set(gcf,'PaperUnits','centimeters','PaperPosition', [0.63, 0.63, ...
        15.0, 7.0]);
191 print(figure(10),'-dpsc','figure/ch4/LEhb.eps')
192
193 %% Efficiency matrix of the heaving two bodies system [kW]
194 figure
195 subplot(1,2,1)
196 contour(H,J*(10^-6),effhtbsL_JH,[0.00001 0.0001 0.001 0.005 0.01 ...
        0.05 0.1 0.2])
197 title('p_{L,\eta_{htbs}}(J,H)')
198 xlabel('H[m]')
199 ylabel('J[MW]')
200
201 subplot(1,2,2)
202 contour(T,J*(10^-6),effhtbsL_JT,[0.00001 0.0001 0.001 0.005 0.01 ...
        0.05 0.1 0.2])
203 title('p_{L,\eta_{htbs}}(J,T)')
204 xlabel('T[s]')
205 ylabel('J[MW]')
206
207 set(gcf, 'PaperType', 'B5')
208 set(gcf,'PaperUnits','centimeters','PaperPosition', [0.63, 0.63, ...
        15.0, 7.0]);
209 print(figure(11),'-dpsc','figure/ch4/LEhtbs.eps')
210
211 %% Efficiency matrix of the pitching device [kW]
212 figure
213 subplot(1,2,1)
214 contour(H,J*(10^-6),effpdL_JH,[0.00001 0.0001 0.001 0.005 0.01 0.05 ...
        0.1 0.2])
215 title('p_{L,\eta_{pd}}(J,H)')
216 xlabel('H[m]')
217 ylabel('J[MW]')
218
```

```
subplot(1,2,2)
contour(T,J*(10^-6),effpdL_JT,[0.00001 0.0001 0.001 0.005 0.01 0.05 ...
    0.1 0.2])
title('p_{L,\eta_{pd}}(J,T)')
xlabel('T[s]')
ylabel('J[MW]')

set(gcf, 'PaperType', 'B5')
set(gcf,'PaperUnits','centimeters','PaperPosition', [0.63, 0.63, ...
    15.0, 7.0]);
print(figure(12),'-dpsc','figure/ch4/LEpd.eps')

%% Efficiency matrix of the floating OWC
figure
subplot(1,2,1)
contour(H,J*(10^-6),efffowcL_JH,[0.00001 0.0001 0.001 0.005 0.01 ...
    0.05 0.1 0.2])
title('p_{L,\eta_{fowc}}(J,H)')
xlabel('H[m]')
ylabel('J[MW]')

subplot(1,2,2)
contour(T,J*(10^-6),efffowcL_JT,[0.00001 0.0001 0.001 0.005 0.01 ...
    0.05 0.1 0.2])
title('p_{L,\eta_{fowc}}(J,T)')
xlabel('T[s]')
ylabel('J[MW]')

set(gcf, 'PaperType', 'B5')
set(gcf,'PaperUnits','centimeters','PaperPosition', [0.63, 0.63, ...
    15.0, 7.0]);
print(figure(13),'-dpsc','figure/ch4/LEfowc.eps')
```

B.1.17 cumulative.m

Calculates the marginal long-term distribution of J, H and T, and the cumulative distribution function.

```

%% Distribution og J

SL_J1=sum(SLJH,2)*delH;
SL_J2=sum(SLJT,2)*delT;

PL_J1=sum(PLJH,2)*delH;
PL_J2=sum(PLJT,2)*delT;

figure
hold on
plot(J*(10^-6),SL_J1,'b-')
plot(J*(10^-6),SL_J2,'r--')
plot(J*(10^-6),PL_J1,'k-')
```

```
15 plot(J*(10^-6),PL_J2,'g--')
16 legend('Scatter diagram (H)','Scatter diagram (T)','Analytical ...
       (H)','Analytical (T)','Location','NorthEast')
17 %title('Distribution of J')
18 xlabel('J[MW]')
19 ylabel('p_L(J)')
20 hold off
21
22 set(gcf, 'PaperType', 'B5')
23 set(gcf,'PaperUnits','centimeters','PaperPosition', [0.63, 0.63, ...
       15.0, 12.0]);
24 print(figure(1),'-dpsc','figure/ch1/pj.eps')
25
26 %% Logharthmic distribution of J
27
28 figure
29 subplot(1,2,1)
30 hold on
31 plot(J(5:32)*(10^-6),SL_J1(5:32),'b-')
32 plot(J(5:32)*(10^-6),SL_J2(5:32),'r--')
33 plot(J(5:32)*(10^-6),PL_J1(5:32),'k-')
34 plot(J(5:32)*(10^-6),PL_J2(5:32),'g--')
35 legend('Sd (H)','Sd (T)','An (H)','An (T)','Location','NorthEast')
36 title('Close-up')
37 xlabel('J[MW]')
38 ylabel('p_L(J)')
39 set(gca, 'xlim', [0.04 0.30001], 'ylim', [0 4.2]);
40 hold off
41
42 subplot(1,2,2)
43 hold on
44 plot(J*(10^-6),log(SL_J1),'b-')
45 plot(J*(10^-6),log(SL_J2),'r--')
46 plot(J*(10^-6),log(PL_J1),'k-')
47 plot(J*(10^-6),log(PL_J2),'g--')
48 legend('Sd (H)','Sd (T)','An (H)','An (T)','Location','NorthEast')
49 title('Logarithmic axis')
50 xlabel('J[MW]')
51 ylabel('ln(p_L(J))')
52 hold off
53
54 set(gcf, 'PaperType', 'B5')
55 set(gcf,'PaperUnits','centimeters','PaperPosition', [0.63, 0.63, ...
       15.0, 7.0]);
56 print(figure(2),'-dpsc','figure/ch1/logpj.eps')
57
58 %% Distribution of H and distribution of T
59 SL_H=sum(SLJH)*delJ*(10^-6);
60 PL_H=sum(PLJH)*delJ*(10^-6);
61
62 SL_T=sum(SLJT)*delJ*(10^-6);
63 PL_T=sum(PLJT)*delJ*(10^-6);
64
65 figure
66 subplot(1,2,1)
67 hold on
68 plot(H,SL_H,'b-')
```

```
plot(H,PL_H,'r-')
legend('Scatter diagram','Analytical','Location','NorthEast')
title('Distribution of H')
xlabel('H[m]')
ylabel('p_L(H)')
hold off

subplot(1,2,2)
hold on
plot(T,SL_T,'b-')
plot(T,PL_T,'r-')
legend('Scatter diagram','Analytical','Location','NorthEast')
title('Distribution of T')
xlabel('T[s]')
ylabel('p_L(T)')
hold off

set(gcf, 'PaperType', 'B5')
set(gcf,'PaperUnits','centimeters','PaperPosition', [0.63, 0.63, ...
    15.0, 7.0]);
print(figure(3),'-dpsc','figure/ch1/phpt.eps')

%% Cumulative distribution fucntion

SLJ1_CDF=zeros(length(J),1);
SLJ2_CDF=zeros(length(J),1);
PLJ1_CDF=zeros(length(J),1);
PLJ2_CDF=zeros(length(J),1);

for i=1:length(J)
    SLJ1_CDF(i)=sum(SL_J1(1:i))*delJ*(10^-6);
    SLJ2_CDF(i)=sum(SL_J2(1:i))*delJ*(10^-6);
    PLJ1_CDF(i)=sum(PL_J1(1:i))*delJ*(10^-6);
    PLJ2_CDF(i)=sum(PL_J2(1:i))*delJ*(10^-6);
end

figure
hold on
plot(J*(10^-6),SLJ1_CDF,'b-')
plot(J*(10^-6),SLJ2_CDF,'r--')
plot(J*(10^-6),PLJ1_CDF,'k-')
plot(J*(10^-6),PLJ2_CDF,'g--')
legend('Scatter diagram (H)','Scatter diagram (T)','Analytical ...
    (H)','Analytical (T)','Location','East')

xlabel('J[MW]')
ylabel('$F_{J}(\hat{J})$','Interpreter','latex')
hold off

set(gcf, 'PaperType', 'B5')
set(gcf,'PaperUnits','centimeters','PaperPosition', [0.63, 0.63, ...
    15.0, 12.0]);
print(figure(4),'-dpsc','figure/ch1/cdfj.eps')
```

B.1.18 fittedcurve.m

Plots the cumulative distribution of J with an exponential distribution and an inverse proportional distribution.

```
1
2  PLJ=SL_J1(1:30);
3  JJJ=J(1:30)*(10^-6);
4
5  PLJ2=55*exp(-50.*JJJ);
6
7  % Plot the curves
8  hold on
9  plot(JJJ,PLJ,'b-')
10 plot(JJJ,PLJ2,'r-')
11 plot(JJJ,1./(5*JJJ),'k-')
12
13 legend('p_L(J)','55*exp(-50*J)','1/(5*J)','Location','NorthEast')
14 xlabel('J[MW]')
15 ylabel('p_L(J)')
16 set(gca, 'xlim', [0 0.30001]);
17
18 set(gcf, 'PaperType', 'B5')
19 set(gcf,'PaperUnits','centimeters','PaperPosition', [0.63, 0.63, ...
       15.0, 12.0]);
20 print(figure(1),'-dpsc','figure/expj.eps')
```

B.1.19 cumuleff.m

Calculates the marginal long-term distribution of power absorption, and the cumulative distribution function for the power absorption.

```
1
2  SLE_Jhb=sum(effhbL_JH,2)*delH;
3  SLE_Jhtbs=sum(effhtbsL_JH,2)*delH;
4  SLE_Jpd=sum(effpdL_JH,2)*delH;
5  SLE_Jfowc=sum(efffowcL_JH,2)*delH;
6
7  figure
8  hold on
9  plot(J(1:20)*(10^-6),SLE_Jhb(1:20),'b-')
10 plot(J(1:20)*(10^-6),SLE_Jhtbs(1:20),'r-')
11 plot(J(1:20)*(10^-6),SLE_Jpd(1:20),'k-')
12 plot(J(1:20)*(10^-6),SLE_Jfowc(1:20),'g-')
13 legend('Heaving buoy','Heaving two bodies system','Pitching ...
       device','Floating OWC','Location','NorthEast')
14 xlabel('J[MW]')
15 ylabel('p_{L,\eta}(J)')
16 hold off
```

```
17
18 set(gcf, 'PaperType', 'B5')
19 set(gcf,'PaperUnits','centimeters','PaperPosition', [0.63, 0.63, ...
       15.0, 12.0]);
20 print(figure(1),'-dpsc','figure/ch4eff/pjeff.eps')
21
22 %% CDF
23 SLE_CDFhb=zeros(length(J),1);
24 SLE_CDFhtbs=zeros(length(J),1);
25 SLE_CDFpd=zeros(length(J),1);
26 SLE_CDFfowc=zeros(length(J),1);
27
28 for i=1:length(J)
29     SLE_CDFhb(i)=   sum(SLE_Jhb(1:i))*delJ*(10^-6);
30     SLE_CDFhtbs(i)= sum(SLE_Jhtbs(1:i))*delJ*(10^-6);
31     SLE_CDFpd(i)=   sum(SLE_Jpd(1:i))*delJ*(10^-6);
32     SLE_CDFfowc(i)= sum(SLE_Jfowc(1:i))*delJ*(10^-6);
33 end
34
35 figure
36 hold on
37 plot(J(1:20)*(10^-6),SLE_CDFhb(1:20),'b-')
38 plot(J(1:20)*(10^-6),SLE_CDFhtbs(1:20),'r-')
39 plot(J(1:20)*(10^-6),SLE_CDFpd(1:20),'k-')
40 plot(J(1:20)*(10^-6),SLE_CDFfowc(1:20),'g-')
41 legend('Heaving buoy','Heaving two bodies system','Pitching ...
       device','Floating OWC','Location','SouthEast')
42 xlabel('J[MW]')
43 ylabel('$F_{J \eta}(\hat{J \eta})$','Interpreter','latex')
44 hold off
45
46 set(gcf, 'PaperType', 'B5')
47 set(gcf,'PaperUnits','centimeters','PaperPosition', [0.63, 0.63, ...
       15.0, 12.0]);
48 print(figure(2),'-dpsc','figure/ch4eff/cdfjeff.eps')
49
50 %% CDF 2
51
52 SLE_CDFhb2=zeros(length(J),1);
53 SLE_CDFhtbs2=zeros(length(J),1);
54 SLE_CDFpd2=zeros(length(J),1);
55 SLE_CDFfowc2=zeros(length(J),1);
56
57 for i=3:length(J)
58
59     SLE_CDFhb2(i)=   sum(SLE_Jhb(3:i))*delJ*(10^-6);
60     SLE_CDFhtbs2(i)= sum(SLE_Jhtbs(3:i))*delJ*(10^-6);
61     SLE_CDFpd2(i)=   sum(SLE_Jpd(3:i))*delJ*(10^-6);
62     SLE_CDFfowc2(i)= sum(SLE_Jfowc(3:i))*delJ*(10^-6);
63 end
64
65 figure
66 hold on
67 plot(J(3:22)*(10^-6),SLE_CDFhb2(1:20),'b-')
68 plot(J(3:22)*(10^-6),SLE_CDFhtbs2(1:20),'r-')
69 plot(J(3:22)*(10^-6),SLE_CDFpd2(1:20),'k-')
70 plot(J(3:22)*(10^-6),SLE_CDFfowc2(1:20),'g-')
```

```
71 legend('Heaving buoy','Heaving two bodies system','Pitching ...
       device','Floating OWC','Location','SouthEast')
72 xlabel('J[MW]')
73 ylabel('$F_{J \eta}(\hat{J \eta})$','Interpreter','latex')
74 hold off
75
76 set(gcf, 'PaperType', 'B5')
77 set(gcf,'PaperUnits','centimeters','PaperPosition', [0.63, 0.63, ...
       15.0, 12.0]);
78 print(figure(3),'-dpsc','figure/ch4eff/cdfjeff2.eps')
```

B.1.20 sizetest.m

Does the size test which is given in chapter 3.3.1 and figure 3.1.

```
1
2  %% Test the size of the calculations
3  tSLJH=zeros(length(J),Xl);
4  sum1=0;
5  sum2=0;
6  sum3=0;
7
8  for i=1:length(J)
9      for j=1:Xl
10         if SLJH(i,j) > 0.08
11             tSLJH(i,j)=3;
12             sum3 = sum3 + SLJH(i,j);
13         elseif SLJH(i,j) > 0.00005
14             tSLJH(i,j)=2;
15             sum2 = sum2 + SLJH(i,j);
16         elseif SLJH(i,j) > 0
17             tSLJH(i,j)=1;
18             sum1 = sum1 + SLJH(i,j);
19         end
20     end
21 end
22
23 sum1=sum1+sum2+sum3;
24 sum2=sum2+sum3;
25
26 tSLJT=zeros(length(J),Xl);
27 tsum1=0;
28 tsum2=0;
29 tsum3=0;
30
31 for i=1:length(J)
32     for j=1:Xl
33         if SLJT(i,j) > 0.05
34             tSLJT(i,j)=3;
35             tsum3 = tsum3 + SLJT(i,j);
36         elseif SLJT(i,j) > 0.00003
37             tSLJT(i,j)=2;
```

```
38              tsum2 = tsum2 + SLJT(i,j);
39          elseif SLJT(i,j) > 0
40              tSLJT(i,j)=1;
41              tsum1 = tsum1 + SLJT(i,j);
42          end
43      end
44  end
45
46  tsum1=tsum1+tsum2+tsum3;
47  tsum2=tsum2+tsum3;
48
49  %% Plot SLJH and SLJT
50  % SLJH
51  figure
52  subplot(1,2,1)
53  h=pcolor(H,J*(10^-6),tSLJH);
54  set(h,'edgecolor','none')
55  title('P_L(J,H)')
56  xlabel('H [m]')
57  ylabel('J [MW]')
58
59  % SLJT
60  subplot(1,2,2)
61  h=pcolor(T,J*(10^-6),tSLJT);
62  set(h,'edgecolor','none')
63  title('P_L(J,T)')
64  xlabel('T [s]')
65  ylabel('J [MW]')
66
67  set(gcf, 'PaperType', 'B5')
68  set(gcf,'PaperUnits','centimeters','PaperPosition', [0.63, 0.63, ...
        15.0, 7.0]);
69  print(figure(1),'-dpsc','figure/allebolger.eps')
70
71  disp(['SLJH, cyan: ' num2str(sum1*delJ*(10^-6)*delH)]);
72  disp(['SLJH, yellow:' num2str(sum2*delJ*(10^-6)*delH)]);
73  disp(['SLJH, red: ' num2str(sum3*delJ*(10^-6)*delH)]);
74
75  disp(['SLJT, cyan: ' num2str(tsum1*delJ*(10^-6)*delT)]);
76  disp(['SLJT, yellow: ' num2str(tsum2*delJ*(10^-6)*delT)]);
77  disp(['SLJT, red: ' num2str(tsum3*delJ*(10^-6)*delT)]);
```

B.2 compare.m

Compares the values obtained from wave scatter diagram and analytical formulas. This script uses the scripts given in appendix B.1.2 and B.1.3.

```
1
2  % Calculates the values analytically
3  analytical;
4
```

```
% Input values for scatter diagram
[blist h t delh delt]=individualwaves;
haltenbanken;

% Calculates the values from the scatter diagram
scattdev;

% Ploting the data
plotfu;

% Results
disp(['area of s_jh: ' num2str(sum(sum(s_jh*delj*delh)))]);
disp(['area of p_jh: ' num2str(sum(sum(p_jh*delj*delh)))]);

disp(['area of s_jt: ' num2str(sum(sum(s_jt*delj*delt)))]);
disp(['area of p_jt: ' num2str(sum(sum(p_jt*delj*delt)))]);

disp(['area of s_HsTp: ' num2str(sum(sum(s_HssTps*delHss*delTps)))]);
disp(['area of p_HsTp: ' num2str(sum(sum(p_HsTp*delHss*delTps)))]);

disp(['area of p_jh: ' num2str(sum(sum(hp_jh*hdelj*hdelh)))]);
disp(['area of p_jt: ' num2str(sum(sum(hp_jt*hdelj*hdelt)))]);
disp(['area of p_HsTp: ' num2str(sum(sum(hp_HsTp*hdelHs*hdelTp)))]);
```

B.2.1 analytical.m

Calculates the analytical formula results with high resolution by also using the scripts given in appendix B.1.7, B.1.8, B.1.9, B.1.10, B.1.11 and B.1.12.

```

%% make highdef graphs
hdelj=0.01;
hjj=hdelj/2:hdelj:4;

hdelh=0.01;
hh=hdelh/2:hdelh:2.9;

hdelt=0.01;
ht=hdelt/2:hdelt:1.85;

hdelHs=0.1;
hHs=hdelHs/2:hdelHs:12.25;

hdelTp=0.1;
hTp=hdelTp/2:hdelTp:22.5;

hp_jh=zeros(length(hjj),length(hh));
hp_jt=zeros(length(hjj),length(ht));
hp_HsTp=zeros(length(hHs),length(hTp));

for m=1:length(hjj)
    for n=1:length(hh)
```

```
24          p_jgh= fp_jgh(hh(n),hjj(m));
25          p_h  = fp_h(hh(n));
26          hp_jh(m,n)  = p_jgh * p_h;
27
28      end
29  end
30
31  for m=1:length(hjj)
32      for n=1:length(ht)
33          p_jkt = fp_jkt (ht(n),hjj(m) );
34          p_tgj = fp_tgj (ht(n),hjj(m) );
35          hp_jt(m,n)  = p_tgj*p_jkt;
36
37      end
38  end
39
40  for m=1:length(hHs)
41      for n=1:length(hTp)
42          p_TpgHs = fp_TpgHs (hHs(m), hTp(n));
43          p_Hs = fp_Hs (hHs(m));
44          hp_HsTp(m,n) = p_TpgHs * p_Hs;
45      end
46  end
```

B.2.2 scattdev.m

Calculates the scatter diagram results, the analytical formula results for the values corresponding to the scatter diagram values, and the deviation between scatter diagram calculations and analytical calculations.

```
1
2
3  %small matrices
4  delj=0.2;
5  jj=delj/2:delj:4;
6  Hs=Hss(:,3);
7  Tp=Tps(3,:);
8
9  %Large matrices
10 % delj=0.2;
11 % jj=delj/2:delj:16;
12 % Hs=Hss(:,3);
13 % Tp=Tps(3,:);
14
15 %% ____________________________
16 s_jh=zeros(length(jj),length(h));
17 s_jt=zeros(length(jj),length(t));
18 p_jh=zeros(length(jj),length(h));
19 p_jt=zeros(length(jj),length(t));
20 s_HssTps=zeros(length(Hss),length(Tps));
21 p_HsTp=zeros(length(Hss),length(Tps));
22
```

```
23 %% p_jh
24 for m=1:length(jj)
25     for n=1:length(h)
26         bjh=0;
27 
28         h1=h(n)-delh/2;
29         h2=h(n)+delh/2;
30         j1=jj(m)-delj/2;
31         j2=jj(m)+delj/2;
32 
33         for o=1:length(blist)
34             bh = blist(o,2);
35             bt = blist(o,3);
36             bj = blist(o,4);
37 
38             if bj >= j1 && bj < j2 % if j-value is in the interval
39                 if bh >= h1 && bh < h2 % if h-value is in the interval
40                     bjh=bjh+1;
41                 end
42             end
43         end
44 
45         s_jh(m,n)=bjh/length(blist)/(delj*delh);
46 
47         p_jgh= fp_jgh(h(n),jj(m));
48         p_h  = fp_h(h(n));
49         p_jh(m,n)  = p_jgh * p_h;
50 
51     end
52 end
53 
54 %% p_jt
55 for m=1:length(jj)
56     for n=1:length(t)
57         bjt=0;
58 
59         t1=t(n)-delt/2;
60         t2=t(n)+delt/2;
61         j1=jj(m)-delj/2;
62         j2=jj(m)+delj/2;
63 
64         for o=1:length(blist)
65             bh = blist(o,2);
66             bt = blist(o,3);
67             bj = blist(o,4);
68 
69             if bj >= j1 && bj < j2 % if j-value is in the interval
70                 if bt >= t1 && bt < t2 % if t-value is in the interval
71                     bjt=bjt+1;
72                 end
73             end
74         end
75 
76         s_jt(m,n)=bjt/length(blist)/(delt*delj);
77 
78         p_jkt = fp_jkt (t(n),jj(m) );
79         p_tgj = fp_tgj (t(n),jj(m) );
```

```
80          p_jt(m,n)   = p_tgj*p_jkt;
81
82      end
83  end
84
85  %% Sea state
86  for m=1:length(Hss)
87      for n=1:length(Tps)
88          s_HssTps(m,n) = B(m,n)/sum(sum(B))/(delHss*delTps);
89
90          p_TpgHs = fp_TpgHs (Hs(m), Tp(n));
91          p_Hs = fp_Hs (Hs(m));
92          p_HsTp(m,n) = p_TpgHs * p_Hs;
93      end
94  end
95
96  err2pjh=(p_jh - s_jh).^2;
97  err2pjt=(p_jt - s_jt).^2;
98  err2pHsTp = (p_HsTp - s_HssTps).^2;
```

B.2.3 plotfu.m

Plots the results calculated by compare.m.

```
1
2  %% Plot
3
4  %% j and h
5  figure
6  subplot(1,3,1)
7  contour(hh,hjj,hp_jh,[0.1 0.2 0.3 0.4 0.5 0.6 0.7 0.8 0.9])
8  title('p(j,h), analytical')
9  xlabel('h')
10 ylabel('j')
11
12 % j and h from scatter
13 subplot(1,3,2)
14 contour(h,jj,s_jh,[0.1 0.2 0.3 0.4 0.5 0.6 0.7 0.8 0.9])
15 title('p(j,h), scatter diagram')
16 xlabel('h')
17 ylabel('j')
18
19 % deviation
20 subplot(1,3,3)
21 contour(h,jj,err2pjh,[0.01 0.1 0.2 0.3 0.4 0.5])
22 title('Deviation')
23 xlabel('h')
24 ylabel('j')
25
26 set(gcf, 'PaperType', 'B5')
27 set(gcf,'PaperUnits','centimeters','PaperPosition', [0.63, 0.63, ...
       15.0, 6.0]);
```

```
28 print(figure(1),'-dpsc','figure/p_jh.eps')
29
30 %% j and t
31 figure
32 subplot(1,3,1)
33 contour(ht,hjj,hp_jt,[0.1 0.25 0.5 0.75 1.0 1.25 1.5 1.75 2])
34 title('p(j,t), analytical')
35 xlabel('t')
36 ylabel('j')
37
38 % j and t from scatter
39 subplot(1,3,2)
40 contour(t,jj,s_jt,[0.1 0.25 0.5 0.75 1.0 1.25 1.5 1.75 2])
41 title('p(j,t), scatter diagram')
42 xlabel('t')
43 ylabel('j')
44
45 % deviation
46 subplot(1,3,3)
47 contour(t,jj,err2pjt,[0.01 0.02 0.03 0.04 0.05 0.1])
48 title('Deviation')
49 xlabel('t')
50 ylabel('j')
51
52 set(gcf, 'PaperType', 'B5')
53 set(gcf,'PaperUnits','centimeters','PaperPosition', [0.63, 0.63, ...
       15.0, 6.0]);
54 print(figure(2),'-dpsc','figure/p_jt.eps')
55
56 %% Hs and Tp
57 figure
58 subplot(1,3,1)
59 contour(hTp,hHs,hp_HsTp,[0.005 0.01 0.02 0.03 0.04 0.05 0.06])
60 title('p(H_s,T_p), analytical')
61 xlabel('Tp')
62 ylabel('Hs')
63
64 % j and t from scatter
65 subplot(1,3,2)
66 contour(Tp,Hs,s_HssTps,[0.005 0.01 0.02 0.03 0.04 0.05 0.06])
67 title('p(H_s,T_p), scatter diagram')
68 xlabel('Tp')
69 ylabel('Hs')
70
71 % deviation
72 subplot(1,3,3)
73 contour(Tp,Hs,err2pHsTp,[0.00001 0.00002 0.00004 0.00005 0.0001])
74 title('Deviation')
75 xlabel('T_p')
76 ylabel('H_s')
77
78 set(gcf, 'PaperType', 'B5')
79 set(gcf,'PaperUnits','centimeters','PaperPosition', [0.63, 0.63, ...
       15.0, 6.0]);
80 print(figure(3),'-dpsc','figure/p_HsTp.eps')
81 % 17 years of education ends with these words that may never be ...
       read and a ring that I hardly gonna use. It was worth it.
```